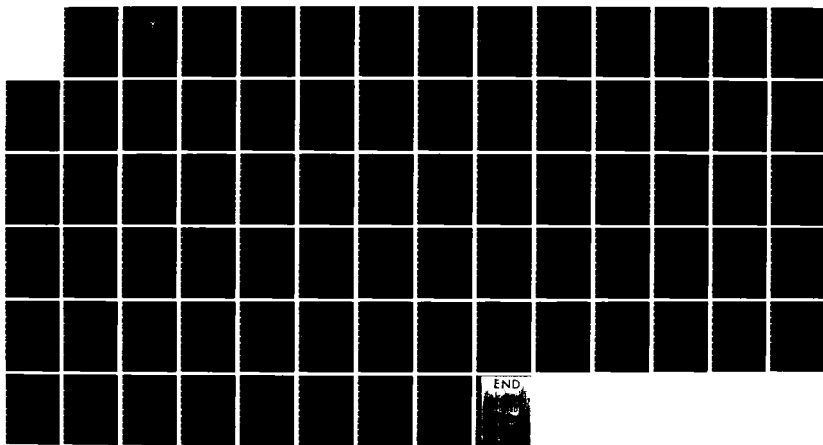AD-A136 794   ORBITAL MOTION OF A FREELY CONING SOLAR SAIL(U) AIR   1/1
               FORCE INST OF TECH WRIGHT-PATTERSON AFB OH SCHOOL OF
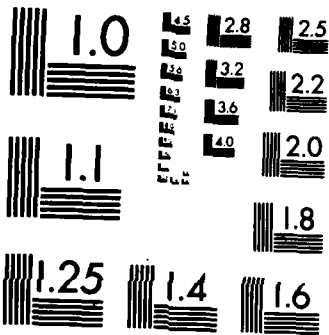   ENGINEERING K L JENKINS DEC 83 AFIT/GA/AA/83D-3
UNCLASSIFIED   F/G 22/3   NL

END

MICROCOPY RESOLUTION TEST CHART

NATIONAL BUREAU OF STANDARDS-1963-A

AIR FORCE INSTITUTE OF TECHNOLOGY

AIR UNIVERSITY
UNITED STATES AIR FORCE

ORBITAL MOTION OF A
FREELY CONING SOLAR SAIL

THESIS

Keith L. Jenkins
First Lieutenant, USAF

AFIT/GA/AA/83D-3

SCHOOL OF ENGINEERING

DTIC
ELECTE
JAN 1 3 1984
E

WRIGHT-PATTERSON AIR FORCE BASE, OHIO

19

AFIT/GA/AA/83D-3

ORBITAL MOTION OF A
FREELY CONING SOLAR SAIL

THESIS

Keith L. Jenkins
First Lieutenant, USAF

AFIT/GA/AA/83D-3

AFIT/GA/AA/83D-3

ORBITAL MOTION OF A FREELY CONING SOLAR SAIL

THESIS

Presented to the Faculty of the School of Engineering

of the Air Force Institute of Technology

Air University

In Partial Fulfillment of the

Requirements for the Degree of

Master of Science in Astronautics

Keith L. Jenkins, B.A., A.A.S., B.S.

First Lieutenant, USAF

December 1983

Acknowledgments

First and foremost, I would like to thank Dr. William Wiesel for his patience, insight and guidance on this project. I would like to thank my wife, Gayle, for her encouragement and support of my efforts, and Lt. and Mrs. Marsh DeHart for their help in preparing the text.

Table of Contents

List of Figures

List of Symbols

A	area of sail.
A'	minor moments of inertia.
a	semimajor axis.
$\hat{b}_i$	body-fixed axes of solar sail.
C	function defined in Appendix A.
C'	moment of inertia about $\hat{b}_3$ axis.
d_i	constants defined in Eq 10.
d/dt	time derivative.
D	sail constant defined in Eq 18.
e	eccentricity.
f	true anomaly.
g	unit conversion constant.
$\hat{H}$	angular momentum vector of sail.
i	inclination.
$\hat{i}, \hat{j}, \hat{k}$	inertia axes.
$\hat{I}, \hat{J}, \hat{K}$	body-centered axes.
n	mean motion.
$R_i()$	vector transformation matrices.
$\hat{s}$	solar direction vector.
s'	solar radiation constant $(4.65 \times 10^{-6}$ N/m.$)$.
t	time.
T	thrust.
τ	period of one orbit.
$\hat{U}, \hat{V}, \hat{W}$	unit vectors in the radial, tangential, and orbit normal directions, respectively.

U,V,W	spacecraft acceleration components in the radial, tangential, and orbit normal directions, respectively.
x	resonance number defined in Eq 38.
α	spin rate of spacecraft about $\hat{b}_3$ axis.
β_i	constants defined in Eqs 13.
γ	angle between $\hat{\omega}$ and $\hat{b}_3$.
Δ	change in orbital parameter.
κ	sail reflectivity constant.
λ	rotation rate of plane defined by $\hat{b}_3$, $\hat{\omega}$, $\hat{H}$.
ζ, η	angular momentum orientation angle.
ν	precession rate.
θ	nutation angle.
μ	gravitational parameter ($1\ DU_\oplus^3/TU_\oplus^2$).
ϕ	phase angle associated with the true anomaly.
ψ	phase angle associated with the sail precession.
ω	argument of periapsis.
$\hat{\omega}$	sail angular velocity vector.
Ω	longitude of the ascending node.

Abstract

This paper addresses orbital perturbations in the two-body problem of an earth-orbiting solar sail undergoing free coning motion in a circular orbit. The coning motion controls both the magnitude and direction of the solar radiation pressure force. The equations of motion are expanded from the Lagrange planetary equations in their acceleration component form and are solved assuming small changes in the orbital elements over the period of one orbit.

Resonances are observed between the mean motion of the sail and its precession rate. The one-to-one resonance case is examined and numerical methods are employed to verify the analytic results for the circular orbit case.

ORBITAL MOTION OF A FREELY CONING SOLAR SAIL

I.   Introduction and Problem Statement

Introduction

Spacecraft propelled by solar radiation pressure are being considered for use in space exploration. Such vehicles require large areas of extremely light-weight, highly reflective sails to convert the linear momentum of sunlight into thrust for the spacecraft. While the acceleration of such a vehicle is quite small, it is continuous, variable, controllable, and does not require the expulsion of mass overboard as with traditional momentum exchange techniques.

Solar sailing vehicles can provide an adequate means of transportation across the long distances typically found in space travel. The force applied to feasible sails is large compared with space drag (Ref 8). While the accelerations of such vehicles are small, the velocity built up over time is substantial. A solar sailing vehicle which can achieve a velocity sufficient to escape the solar system is feasible (Ref 4). Escape from Earth orbit is possible after a month or two (Ref 4). The solar sail has the additional advantage of simplicity of design when compared with other low-thrust propulsion systems (Ref 8).

In attempts to determine the best steering program for solar sails, a variety of approaches have been tried. Garwin (Ref 4) began the investigations with a sail that could be furled when sailing into the Sun's rays, and unfurled when sailing with the solar flux. This is similar to a method proposed by Van der Ha and Modi (Ref 9) which involved "on-off switching". London (Ref 6) sought the one best constant angle for a given mission. A more advanced method was introduced by Fimple (Ref 3) who determined a steering program based on the time rate of change of energy increase. All of these approaches have in common that if the sail is rotated at all it is rotated with the angular momentum vector coinciding with a body axis of symmetry, i.e., spinning. This article represents a departure from this traditional approach.

The question is, essentially, how to best control the thrust of a solar sailing vehicle. Because of the inherent flimsiness of light-weight sails, quick maneuvers are not possible with solar sailing vehicles. Looked at another way, if a method can be found which both provides adequate performance and restricts the sail to smooth rotations, then the necessary structural strength and weight of the sails can be minimized. Adequate performance is defined in terms of the spacecraft's ability to increase the semimajor axis of its orbit and to change the inclination of its orbit. Specific performance criteria depend on mission

requirements. Control of the coning motion would be accomplished by control of the magnitude of the angular momentum vector.

This work uses techniques pioneered in Capt Salvatore Alfano's thesis: "Low Thrust Orbit Transfer" (Ref 1). For those not familiar with the work, the consideration of orbital changes for very low thrust vehicles is broken into two parts. The first part is a fast timescale problem in which many orbital parameters can be considered constant over one orbit, the perturbations being found and added at the end of the orbit. The second part is a slow timescale problem in which many perturbed orbits are linked to achieve a transfer. What follows here is the derivation and examination of the equations for the fast timescale problem for solar sails.

Problem Statement

The objective is to derive the perturbation equations for an earth-orbiting solar sail which is undergoing a coning motion. The sail is modeled as a flat, rigid, plate which is undergoing the free coning motion of an axisymmetric rigid body. During the course of one orbit, the sail is considered to be torque free. The earth is modeled as a point mass. Because of the low thrust of the vehicle, only small changes in the orbit are possible.

- 3 -

Thus, the semimajor axis (a), inclination (i), eccentricity (e), argument of periapsis (ω), and the longitude of the ascending mode (Ω) are considered constant over the orbit and then updated.

The perturbation equations are to be examined analytically to determine what, if any, important resonances arise. A promising resonance case will be examined.

II.   Attitude Dynamics of a Freely Coning Solar Sail

Fundamentals of Coning Motion

The attitude motion of the sail is that of the freely
coning motion of an axisymmetric body. The body is a flat,
rigid, plate which exhibits perfectly specular reflection on
both sides. A review of the fundamentals of free coning
motion is appropriate.

Coning   motion   is   the   motion   of   a   torque   free
axisymmetric rigid body in the case where the angular
velocity vector, $\hat{\omega}$, is not colinear with the angular
momentum vector, $\hat{H}$. The assumption that the body is torque
free implies that $\hat{H}$ is constant in direction and magnitude.
It has been shown (Ref 5) that $\hat{H}$ is coplanar with $\hat{\omega}$ and a
vector along the body's axis of symmetry, $\hat{b}_3$. Furthermore,
since the orientation of the angular momentum vector is
constant in inertial space, the plane which contains the
three vectors rotates about the angular momentum vector (Fig
1). We can designate the angle between $\hat{H}$ and $\hat{b}_3$ as   the
nutation angle, θ, which is constant. A second angle, γ ,
is the angle between $\hat{\omega}$ and $\hat{b}_3$. This plane rotates with a
constant angular velocity λ. As the vector plane rotates,
describes a space cone around $\hat{H}$. This cone remains fixed in
inertial space and a cone defined by $\hat{b}_3$ and $\hat{\omega}$ rolls without
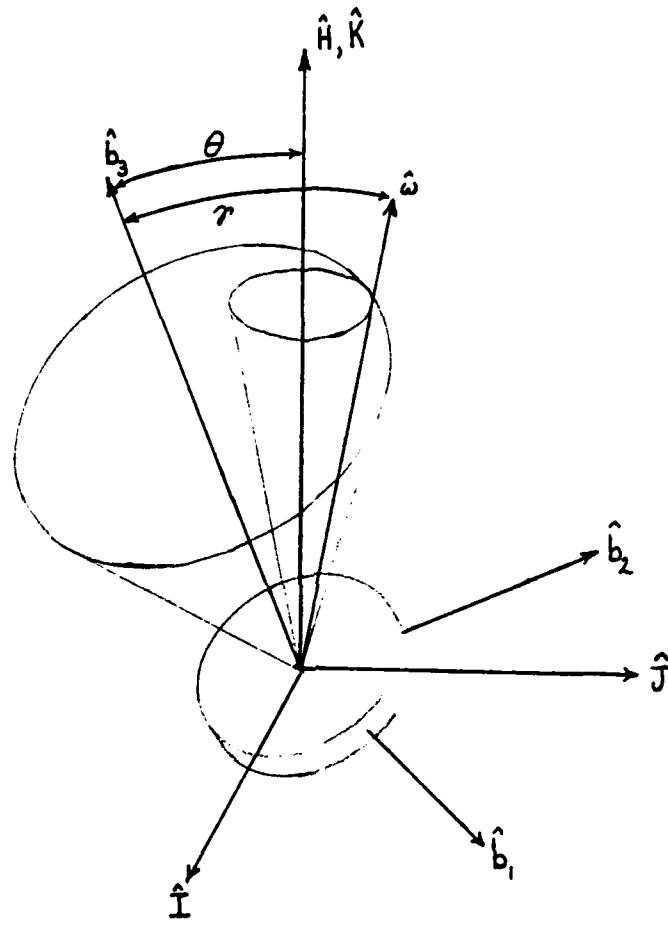slipping on the space cone. For a body with moments of

Fig 1.   Coning Motion Parameters

inertia A', A' and C', where C' is the moment of inertia about $\hat{b}_3$, the following relationship applies (Ref 5):

$$\tan\theta = \frac{A'}{C'}\tan\gamma$$

(1)

For cases where C' > A', this implies that $\gamma > \theta$, as shown in Figure 1.

Consider that $\hat{H}$ is colinear with an inertial reference axis, $\hat{K}$, and that the $\hat{I}$ and $\hat{J}$ axes form a right-handed orthogonal set with $\hat{K}$ (Fig 2). Consider also a projection of $\hat{b}_3$ onto the $\hat{I},\hat{J}$ plane. This projection will rotate about $\hat{K}$ and, therefore, about $\hat{H}$ at the constant precession rate ν given by:

$$\nu = C'\alpha / (A' - C')\cos\theta$$

(2)

where α is the angular velocity of the body about the $\hat{b}_3$ axis (Ref 5). For ν to be positive in the case where C' > A', α must be negative. Since α is just the spin of the plate about its axis of symmetry, this presents no difficulty.

The main points of interest are that the precession rate, nutation angle, and the angular momentum vector are all constant. These facts provide the basis for
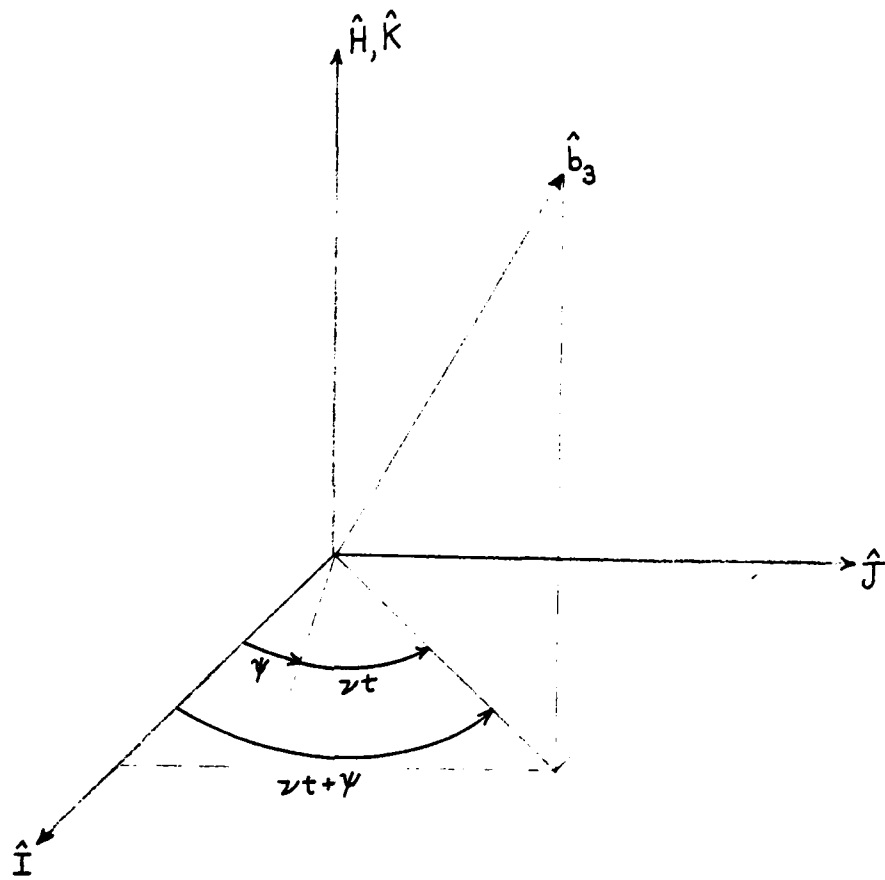
Fig 2. Precession Rate

determination of the magnitude and direction of the thrust vector. From this general groundwork, specific equations for the attitude motion of the solar sail can be found.

Attitude Motion of the Sail

The solar sail is a flat plate, perfectly specularly reflective on both sides and with moments of inertia A', A', and C'. C' is the major axis of inertia and lies perpendicular to the plane of the sail. The body axes of the sail are designated $\hat{b}_3$, $\hat{b}_2$, and $\hat{b}_1$, where $\hat{b}_1$ and $\hat{b}_2$ are axes about which the moments of inertia are A', and $\hat{b}_3$ is the axis about which the moment of inertia is C'. (See Fig 3.)

The original orbit plane will be considered inertial. The inertial axes will be designated $\hat{i}$, $\hat{j}$, and $\hat{k}$ where $\hat{k}$ is normal to the orbit plane, $\hat{i}$ is in the orbit plane and in a plane perpendicular to the ecliptic and containing the Earth-Sun line, and $\hat{j}$ forms a right-handed orthogonal set as in Fig 4. The angle between the first point of Aries and the Earth-Sun line is considered to be constant over one orbit.

Both the magnitude and direction of the thrust are functions of time. The magnitude in the $-\hat{b}_3$ direction is simply:
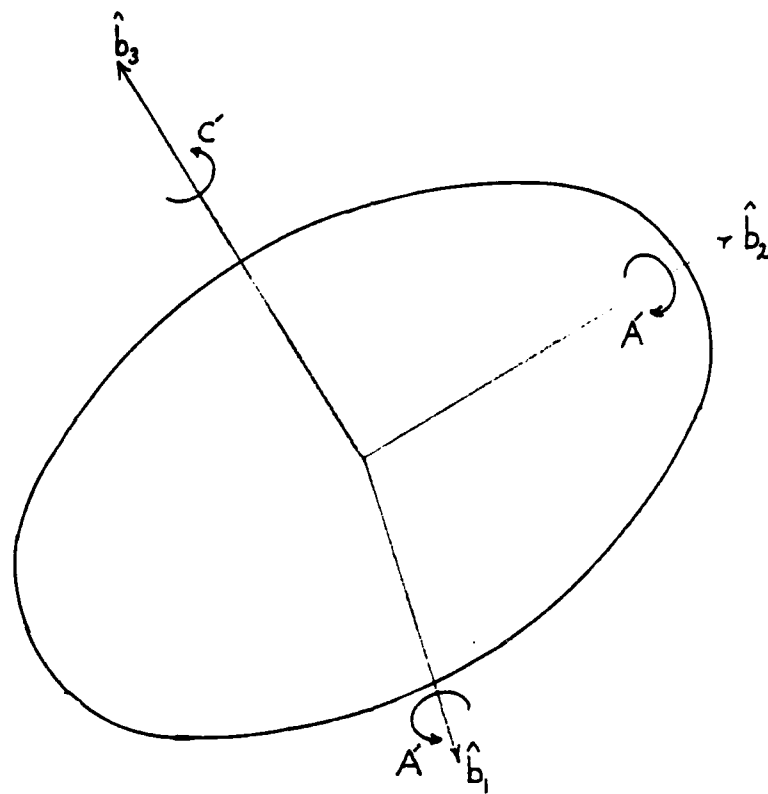
Fig 3. Solar Sail Body Axes and Moments of Inertia
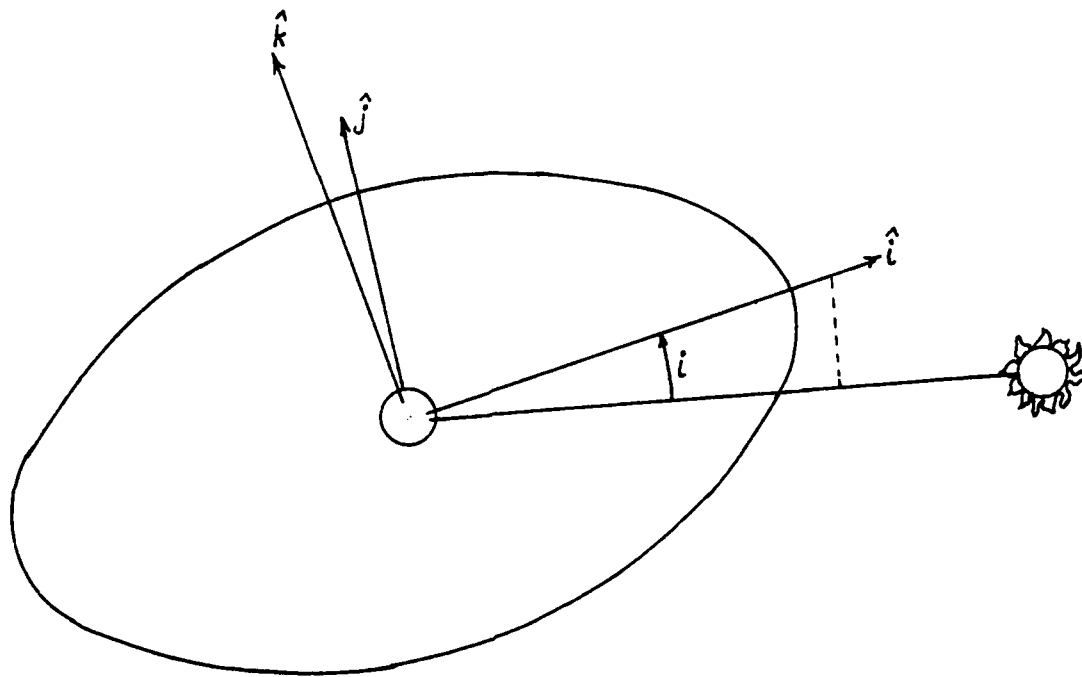
Fig 4. $\hat{i}, \hat{j}, \hat{k}$ Reference Frame
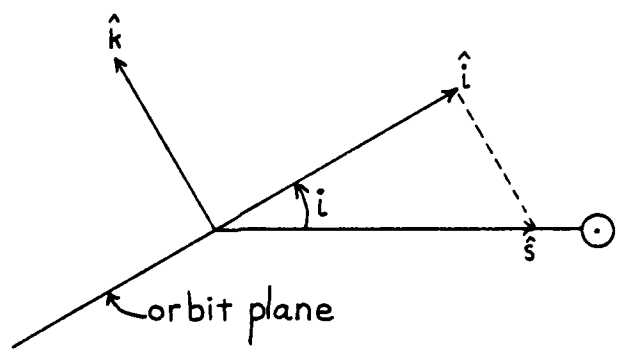
Fig 5. Definition of $\hat{s}$

$$T = s K A g (\hat{b}_3 \cdot \hat{s})^2 \qquad (3)$$

where s is the solar constant, K is a sail parameter dependent upon the reflectivity and transmissivity of the sail, A is the area of the sail, $A(\hat{b} \cdot \hat{s})$ is the projected area of the sail on a plane perpendicular to the Sun's rays, and g is the unit conversion factor. The unit vector $\hat{s}$, shown in Fig 5, gives the direction of the Sun and is defined by

$$\hat{s} = \cos i \, \hat{i} - \sin i \, \hat{k} \qquad (4)$$

The definition of i used here and shown in Fig 4 implies that Ω is fixed at a negative one-half pi radians from the $\hat{i}$ axis. There is great simplification in this choice, and little loss of generality for the current problem. The maximum change in inclination can still be seen.

The direction of the thrust is $-\hat{b}_3$, assuming that $\hat{b}_3$ is on the sunward side of the sail. Since i, $\hat{i}$, $\hat{k}$, s, K and A are known and constant over one orbit it remains only to find $\hat{b}_3$ expressed in terms of functions of time.

Given that the angular momentum vector $\hat{H}$ has an arbitrary orientation in inertial space, we can define a

coordinate system $\hat{I}$, $\hat{J}$, $\hat{K}$ such that $\hat{K}$ is along $\hat{H}$, $\hat{I}$ is perpendicular to $\hat{H}$ and lies in the $\hat{i}, \hat{j}$ plane, and $\hat{J}$ forms a right-handed orthogonal set. This permits the definition of $\hat{H}$ by means of two angles of rotation ζ and η, as shown in Figure 6 (Ref 10). Any vector in this $\hat{I}$, $\hat{J}$, $\hat{K}$ frame can be expressed in the $\hat{i}$, $\hat{j}$, $\hat{k}$ inertial frame by the transformation

$$\begin{Bmatrix} i \\ j \\ k \end{Bmatrix} = R_3(-\zeta) R_1(-\eta) \begin{Bmatrix} I \\ J \\ K \end{Bmatrix} \tag{5}$$

where

$$R_1(x) \begin{bmatrix} 1 & 0 & 0 \\ 0 & \cos x & \sin x \\ 0 & -\sin x & \cos x \end{bmatrix} \quad R_3(x) \begin{bmatrix} \cos x & \sin x & 0 \\ -\sin x & \cos x & 0 \\ 0 & 0 & 1 \end{bmatrix} \tag{6}$$

The unit vector $\hat{b}_3$ is defined in the $\hat{I}$, $\hat{J}$, $\hat{K}$ frame shown in Fig 7. This leads to an expression for $\hat{b}_3$ in the form:

$$\hat{b}_3 = \sin\theta\cos(\nu(t-t_0))\hat{I} + \sin\theta\sin(\nu(t-t_0))\hat{J} + \cos\theta\hat{K} \tag{7}$$
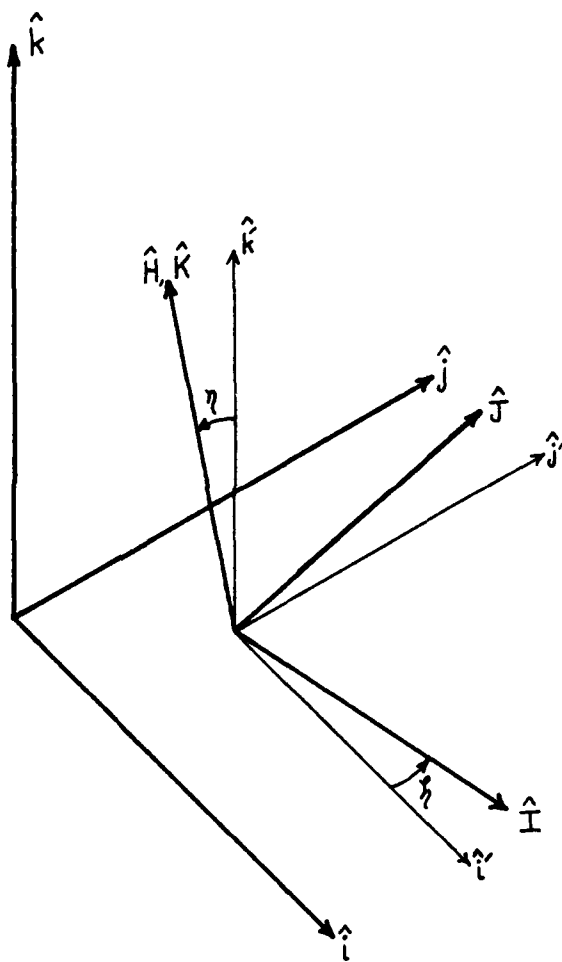
Fig 6. Orientation Angles for $\hat{H}$
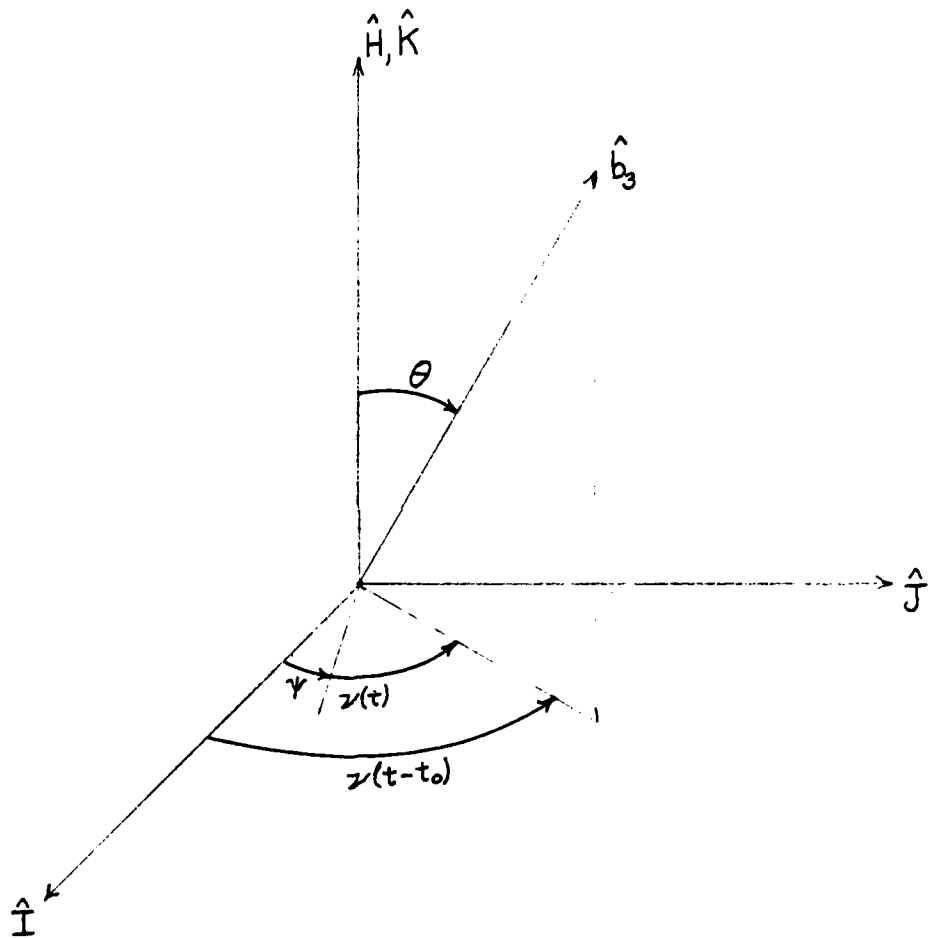
Fig 7. Unit Vector $\hat{b}_3$

The nutation angle θ is a constant over one orbit. The precession angle $\nu(t-t_o)$ is obviously a function of time. For simplicity, t_o is set at zero and a phase angle, γ, is used to offset the starting point away from the $\hat{I}$ axis when desirable. As will be seen, phase angles are crucial because a given coning motion can create different effects depending on initial conditions.

To get thrust magnitude we need $(\hat{b}_3 \cdot \hat{s})$ which leads to the necessity of expressing $\hat{b}_3$ in terms of the $\hat{i}$, $\hat{j}$, $\hat{k}$ reference. This is accomplished by transformation Eq 5, resulting in

$$\hat{b}_3 \begin{Bmatrix} i \\ j \\ k \end{Bmatrix} = \begin{Bmatrix} s\theta c\nu t c\eta - s\theta s\nu t c\eta s\eta + c\theta s\eta s\eta \\ s\theta c\nu t s\eta + s\theta s\nu t c\eta c\eta - c\theta s\eta c\eta \\ s\theta s\nu t s\eta + c\theta c\eta \end{Bmatrix} \qquad \begin{aligned} s &\equiv \sin \\ c &\equiv \cos \end{aligned} \qquad (8)$$

which implies that

$$\hat{b}_3 \cdot \hat{s} = d_1 \cos(\nu t + \gamma) - d_2 \sin(\nu t + \gamma) + d_3 \qquad (9)$$

where constants d_1, d_2, and d_3 are defined by:

$$d_1 = \sin\theta \cos\eta \cos i$$

$$d_2 = \sin\theta\cos\eta\sin\hbar\cos i + \sin\theta\sin\eta\sin i$$

$$d_3 = \cos\theta\sin\eta\sin\hbar\cos i - \cos\theta\cos\eta\sin i \tag{10}$$

It is convenient to define a set of axes with their origin at the center of mass of the spacecraft and with axes $\hat{U}$, $\hat{V}$, and $\hat{W}$ in the orbit radial, tangential, and normal directions, respectively. To get the direction of the thrust, $\hat{b}_3$ must be expressed in the $\hat{U}$, $\hat{V}$, $\hat{W}$ reference frame. This is accomplished by noting Figure 8 and writing the transformation

$$\begin{Bmatrix} U \\ V \\ W \end{Bmatrix} = R_3(f)\begin{Bmatrix} i \\ j \\ k \end{Bmatrix} = R_3(f)R_3(-\hbar)R_1(-\eta)\begin{Bmatrix} I \\ J \\ K \end{Bmatrix} \tag{11}$$

where f is the true anomaly and ϕ is a phase angle.

Transformation (11) results in

$$\hat{b}_3\begin{Bmatrix} U \\ V \\ W \end{Bmatrix} = \begin{Bmatrix} \beta_1 cvcf - \beta_2 svcf + \beta_3 cf + \beta_4 cvsf + \beta_5 svsf + \beta_6 sf \\ -\beta_1 cvsf + \beta_2 svsf - \beta_3 sf + \beta_4 cvcf + \beta_5 svcf + \beta_6 cf \\ \beta_7 sv + \beta_8 \end{Bmatrix}$$

$$s \equiv \sin, \quad c \equiv \cos, \quad v \equiv \nu t + \gamma, \quad f \equiv nt + \phi \tag{12}$$

where the constants β_1 through β_8 are defined by:
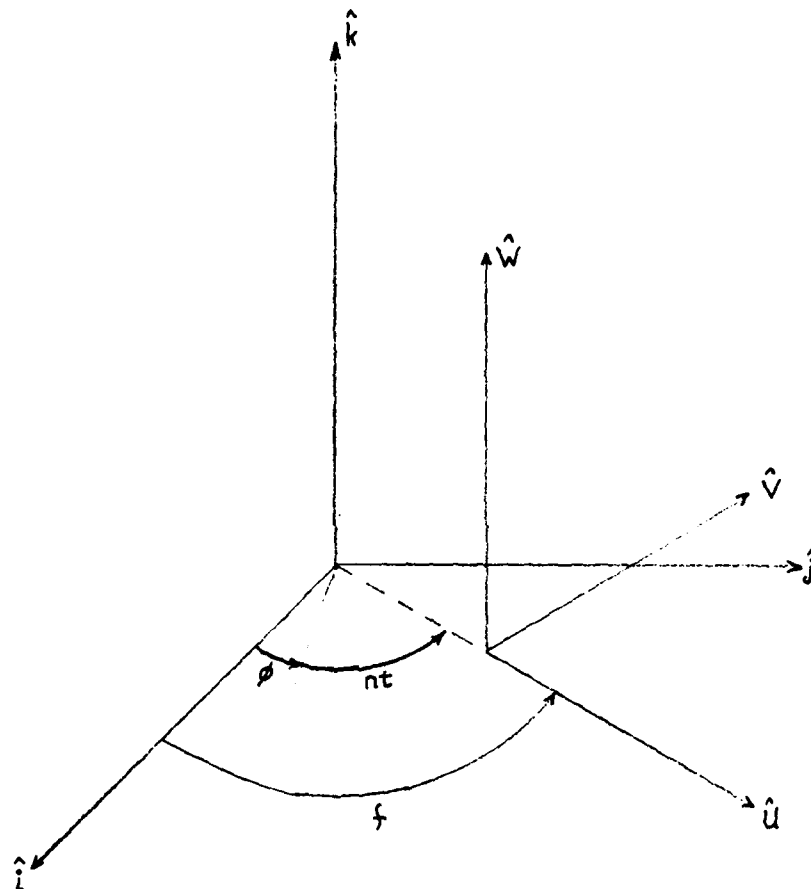
Fig 8. $\hat{i}, \hat{j}, \hat{k}$, to $\hat{U}, \hat{V}, \hat{W}$ Transformation

$$\beta_1 = \sin\theta\cos\zeta$$

$$\beta_2 = \sin\theta\cos\eta\sin\zeta$$

$$\beta_3 = \cos\theta\sin\eta\sin\zeta$$

$$\beta_4 = \sin\theta\sin\zeta$$

$$\beta_5 = \sin\theta\cos\eta \qquad\qquad (13)$$

$$\beta_6 = \cos\theta\sin\eta\cos\zeta$$

$$\beta_7 = \sin\theta\sin\eta$$

$$\beta_8 = \cos\theta\cos\eta$$

These results provide the accelerations in the radial, tangential, and orbit normal directions. Remembering Newton's Second Law:

$$F = ma \implies a = F/m \qquad\qquad (14)$$

then

$$U = T/m = D\,(\hat{b}_3 \cdot \hat{s})^2(\hat{b}_3 \cdot \hat{U}) \qquad\qquad (15)$$

$$V = T/m = D(\hat{b}_3 \cdot \hat{s})^2(\hat{b}_3 \cdot \hat{V}) \qquad (16)$$

$$W = T/m = D(\hat{b}_3 \cdot \hat{s})^2(\hat{b}_3 \cdot \hat{W}) \qquad (17)$$

and let

$$D = s\hbar Ag/m \qquad (18)$$

be called the sail constant, where g is the unit conversion factor. The components of acceleration in the radial (U), tangential (V), and orbit normal (W) directions are now known, along with the magnitude of the thrust (T).

III. The Orbital Equations of Motion

The objective is to develop the orbital equations of motion from the Lagrange planetary equations in their acceleration component form. The Lagrangian equations are:

$$\frac{da}{dt} = \frac{2Ue\sin f}{n(1-e^2)^{1/2}} + \frac{2V(1+e\cos f)}{n(1-e^2)^{1/2}} \tag{19}$$

$$\frac{di}{dt} = \frac{W\cos(f+\omega)(1-e^2)^{1/2}}{na(1+e\cos f)} \tag{20}$$

$$\frac{d\Omega}{dt} = \frac{W\sin(f+\omega)(1-e^2)^{1/2}}{na(1+e\cos f)\sin i} \tag{21}$$

$$\frac{d\omega}{dt} = \frac{-U\cos f(1-e^2)^{1/2}}{nae} + \frac{V(1-e^2)^{1/2}(2+e\cos f)\sin f}{nae(1+e\cos f)}$$

$$\frac{-W\sin(f+\omega)\cot i(1-e^2)^{1/2}}{na(1+e\cos f)} \tag{22}$$

$$\frac{de}{dt} = \frac{U(1-e^2)^{1/2}\sin f}{na}$$

$$+ \frac{V(1-e^2)^{1/2}}{nae}\left[1+e\cos f - \frac{1-e^2}{1+e\cos f}\right] \tag{23}$$

- 21 -

where U, V, and W are the spacecraft accelerations in the radial, tangential, and orbit normal directions and n is the mean motion. The true anomaly is designated f and consists of

$$f = n(t - t_o) + \phi \qquad (24)$$

where t_o will be taken to be zero and ϕ is a phase angle between the $\hat{i}$ axis and the beginning of the orbit.

For circular orbits, ω is arbitrarily set to zero, and the time derivative of the argument of periapsis is undefined. This reduces the number of equations of motion to four. Simplifying for e equals zero we get:

$$\frac{da}{dt} = \frac{2V}{n} \qquad (25)$$

$$\frac{de}{dt} = \frac{U \sin f}{na} + \frac{2V \cos f}{na} \qquad (26)$$

$$\frac{di}{dt} = \frac{W \cos f}{na} \qquad (27)$$

$$\frac{d\Omega}{dt} = \frac{W \sin f}{na \sin i}$$

(28)

Substituting Eqs 15-17 into Eqs 25-28 results in:

$$\frac{da}{dt} = \frac{2D(\hat{b}_3 \cdot \hat{s})^2 (\hat{b}_3 \cdot \hat{V})}{n}$$

(29)

$$\frac{de}{dt} = \frac{U(\hat{b}_3 \cdot \hat{s})^2 (\hat{b}_3 \cdot \hat{U}) \sin f + 2D(\hat{b}_3 \cdot \hat{s})^2 (\hat{b}_3 \cdot \hat{V}) \cos f}{na}$$

(30)

$$\frac{di}{dt} = \frac{D(\hat{b}_3 \cdot \hat{s})^2 (\hat{b}_3 \cdot \hat{W}) \cos f}{na}$$

(31)

$$\frac{d\Omega}{dt} = \frac{D(\hat{b}_3 \cdot \hat{s})^2 (\hat{b}_3 \cdot \hat{W}) \sin f}{na \sin i}$$

(32)

These are the orbital equations of motion for the freely coning solar sail in the Lagrangian acceleration component form.

To obtain the changes in orbital parameters, Eqs 29-32 are integrated with respect to time over one orbit, the period being determined from

$$T = 2\pi a^{3/2}\mu^{-1/2} \tag{33}$$

Perturbation Solutions

To obtain the general perturbation solution for the orbit of a freely coning solar sail, Eqs 9 and 12 are substituted into Eqs 29-32 which are integrated with respect to time between the limits zero and T. Since these equations contain both f and ν which are functions of time, the perturbations solutions are quite lengthy. For this reason they have been placed in Appendix A. The reader is strongly urged to examine them in some detail before proceeding. The perturbation equations are given here in abbreviated form for notational clarity:

$$\Delta a = \int_0^T \frac{da}{dt}\, dt \tag{34}$$

$$\Delta e = \int_0^T \frac{de}{dt}\, dt \qquad (35)$$

$$\Delta i = \int_0^T \frac{di}{dt}\, dt \qquad (36)$$

$$\Delta \Omega = \int_0^T \frac{d\Omega}{dt}\, dt \qquad (37)$$

IV. Resonances

Inspection of the equations in Appendix A indicate the presence of resonances. These appear as terms in the denominators which could go to zero if the correct relationship between ν and n existed. When a resonance condition is met, the term in which the resonance occurs becomes large. This is the key to maximizing the small changes in the orbital elements, which is our objective.

Several different resonances occur in the perturbation solutions. In order to more easily select useful resonances, all resonances have been displayed in Tables I-IV. The resonances are given in the form:

$$\nu = x n \tag{38}$$

where x is the resonance number given in the table. The tables display the resonances in a grid which indicates which constants each resonance affects. For instance, the one-to-one resonance enlarges the constants β_1, β_2, β_4, and β_5, each multiplied by the constant d_3^2, in the $\triangle a$ equation. A negative sign beside a resonance number means that this term tends to reduce the perturbation, assuming both phase angles (ϕ & γ) are zero. Adjustment of the phase angles can change the sign of a given term. Using these

TABLE I

Resonance terms in a

(Constants)	$2d_1 d_3$	$2d_2 d_3$	d_3^2
β_1	$-1/2$	$1/2$	-1
β_2	$1/2$	$1/2$	1
β_3	-1	1	0
β_4	$1/2$	$1/2$	1
β_5	$-1/2$	$1/2$	-1
β_6	1	1	0

(Constants)	d_1^2	$2d_1 d_2$	d_2^2
β_1	$-1,\ -1/3$	$1,\ 1/3$	$-1,\ 1/3$
β_2	$1,\ 1/3$	$-1,\ 1/3$	$1,\ -1/3$
β_3	$-1/2$	$1/2$	$1/2$
β_4	$1,\ 1/3$	$1,\ 1/3$	$1,\ -1/3$
β_5	$-1,\ -1/3$	$-1,\ 1/3$	$-1,\ 1/3$
β_6	$1/2$	$1/2$	$-1/2$

TABLE II

Resonance terms in e

(Constants)	d_1^2	$2d_1 d_2$	d_2^2
β_1	-2, -2/3	2, 2/3	-2, 2/3
β_2	2, 2/3	-2, 2/3	2, -2/3
β_3	-1	1	1
β_4	2, 2/3	2, 2/3	2, -2/3
β_5	-2, -2/3	-2, 2/3	-2, 2/3
β_6	1 *	1	-1 *

(Constants)	$2d_1 d_3$	$2d_2 d_3$	d_3^2
β_1	-1	1	-2
β_2	1	1	2
β_3	-2	2	0
β_4	1 *	1	2
β_5	-1	1 *	-2
β_6	2	2	0 *

TABLE III

Resonance terms in $\dot{\imath}$

(Constants)	d_1^2	$2d_1 d_2$	d_2^2
β_7	$-1,\ -1/3$	$-1,\ 1/3$	$-1,\ 1/3$
β_8	$1/2$	$1/2$	$-1/2$

(Constants)	$2d_1 d_3$	$2d_2 d_3$	d_3^2
β_7	$1/2$	$1/2$	-1
β_8	1	1	0

TABLE IV

Resonance terms in

(Constants)	d_1^2	$2d_1 d_2$	d_2^2
β_7	$1,\ 1/3$	$-1,\ 1/3$	$1,\ -1/3$
β_8	$1/2$	$1/2$	$-1/2$

(Constants)	$2d_1 d_3$	$2d_2 d_3$	d_3^2
β_7	$1/2$	$1/2$	1
β_8	1	-1	0

tables, a useful resonance can be chosen.

One-to-One Resonance Case

The perturbation solutions for the one-to-one resonance case, integrated over one orbital period, are given here.

$$\Delta a = a^{3/2} DT \{ (d_1^2/4)\{ (\beta_2 + 3\beta_4)\cos(\phi-\gamma) - (3\beta_1 + \beta_5)\sin(\phi-\gamma)\}$$
$$- (d_1 d_2/2)\{ (\beta_2 - \beta_4)\sin(\phi-\gamma) + (\beta_5 - \beta_1)\cos(\phi-\gamma)\} + 2 d_1 d_3 \{$$
$$\beta_6 \cos(\phi-\gamma) - \beta_3 \sin(\phi-\gamma)\} + 2 d_2 d_3 \{ \beta_3 \cos(\phi-\gamma) + \beta_6 \sin(\phi-\gamma)\}$$
$$+ (d_2^2/4)\{ (3\beta_2 + \beta_1)\cos(\phi-\gamma) - (\beta_1 + 3\beta_5)\sin(\phi-\gamma)\} +$$
$$d_3^2 \{ (\beta_2 + \beta_4)\cos(\phi-\gamma) - (\beta_1 + \beta_5)\sin(\phi-\gamma)\} \}$$

(39)

$$\Delta e = (a^{1/2} DT/8) \{ d_1^2 \{ -\beta_3 \sin(2(\phi-\gamma)) + \beta_6 (6 + \cos(2(\phi-\gamma)))\}$$
$$+ 2 d_1 d_2 \{ \beta_3 \cos(2(\phi-\gamma)) + \beta_6 \sin(2(\phi-\gamma))\} + d_2^2 \{ \beta_3 \sin(2(\phi-\gamma))$$
$$+ \beta_6 (6 - \cos(2(\phi-\gamma)))\} + 2 d_1 d_3 \{ (\beta_2 + \beta_4)\cos(2(\phi-\gamma)) - (\beta_1 +$$
$$\beta_5)\sin(2(\phi-\gamma)) + 6\beta_4\} + 2 d_2 d_3 \{ (\beta_2 + \beta_4)\sin(2(\phi-\gamma)) + (\beta_1$$
$$+ \beta_5)\cos(2(\phi-\gamma)) - 6\beta_5\} + 12 d_3^2 \beta_6\}$$

(40)

$$\Delta i = (a^{1/2} DT/2) \{ 2 d_3 \beta_8 \{ d_1 \cos(\phi-\gamma) + d_2 \sin(\phi-\gamma)\} -$$
$$\beta_7 \{ [(d_1^2/4) + (3 d_2^2/4) + d_3^2] \sin(\phi-\gamma) + (d_1 d_2/2)\cos(\phi-\gamma)\} \}$$

(41)

- 30 -

$$\Delta \Omega = (a^{1/2} DT / 2 \sin i) \{ \beta_7 \{ [(d_1^2 / 4) + (3 d_2^2 / 4) + d_3^2] \cos (\phi - \gamma)$$
$$- (d_1 d_2 / 2) \sin (\phi - \gamma) \} + 2 \beta_8 d_3 \{ d_1 \sin (\phi - \gamma) - d_2 \cos (\phi - \gamma) \} \}$$

(42)

The one-to-one resonance case has several interesting properties. First, it the most frequently encountered resonance case in the Δa, Δi, and $\Delta \Omega$ equations. Since the performance requirement is to have a large change in the semimajor axis and/or the inclination, the one-to-one resonance case is preferred. Secondly, when the one-to-one resonance is selected and the integration is taken over one orbital period, i.e.,

$$nT = 2 \pi$$

(43)

then virtually all terms not containing a one-to-one resonance disappear. The only exception is the last term in the Δe equation which, along with four other Δe terms which are one-to-one resonant, cannot be integrated to zero under any circumstances. These five terms are non-periodic and can be eliminated only by proper selection of constant angles. Non-periodic terms occur only in the Δe equation

and are indicated by an asterisk in Table II.

Thirdly, the one-to-one resonance case is the only integer resonance case in the $\triangle a$, $\triangle i$, and $\triangle \Omega$ equations. To integrate non-resonance terms to zero for the fractional resonances requires a period of more than one orbit. This limits the orbits for which the perturbation assumptions are valid to smaller semimajor axes than for the one-to-one resonance case. Conversely, if one orbit is taken as the upper limit of integration, none of the terms would be eliminated and the simplicity of the analytic method would be destroyed.

Other Resonances

The two-to-one resonance case changes e only. In the event that the mission objective involves changing the eccentricity only, this would be the resonance of choice. Because of the circular orbit assumptions, this case is not investigated further here.

The one-half-to-one resonance case would be the secondary choice for changing a and i, but it should be noted that the two-to-one resonance terms in $\triangle e$ do not integrate to zero in this case. Thus, no advantage over the one-to-one case is evident.

The one-third-to-one resonance case will eliminate the

two-thirds-to-one resonance terms in $\triangle e$ and vise versa. However, either choice results in no resonance terms in $\triangle i$ or $\triangle \Omega$, which contradicts the performance objectives.

Any integer resonance above two-to-one results in nearly all changes being equal to zero over one orbit. The five terms in $\triangle e$ which cannot be integrated to zero can be set to zero by appropriate choice of orientation angles. These resonances, then, represent orbit-keeping strategies. Consequently, they are not of interest for present purposes.

A consideration of specific cases is provided in the next chapter.

V. Results and Discussion

Results

For the single resonance case, many cases were tested, ranging from the trivialy simple to the arbitrarily complicated. These cases were tested by numerically integrating Eqs 29-32 and comparing the results with the analytic solutions, Eqs 39-42. The numerical integration was accomplished using a predictor-corrector technique contained in a subroutine Haming, contained in Appendix B. The Earth-Canonical system of units was used and a value of D was taken as 4.65 E-06. For the test cases, the semimajor axis was taken to be five $DU_{\oplus}$.

Motion in the Ecliptic Plane.

The most trivial cases are those in which the inclination is zero. This leaves the longitude of the ascending node undefined, and the problem reduces to three equations.

Spinning. The simplest case is the one in which $\hat{H}$ is parallel to $\hat{k}$, and the nutation angle is one-half pi radians. This leads to the analytical expressions:

$$\triangle a = -a^{3/2}DT\sin(\phi-\gamma) \qquad (44)$$

$$\triangle e = \triangle i = 0 \qquad (45)$$

Obviously, the maximum change in $\triangle a$ is when

$$\phi - \gamma = -\pi/2 \qquad (46)$$

This is verified in Fig 9, where the line represents the change in $\triangle a$ over time and the "x" indicates the point predicted by Eq 44.

Tumbling. Tumbling is simply spinning with $\hat{H}$ parallel to $\hat{j}$ or $\hat{i}$. The case of $\hat{H}$ parallel to $\hat{i}$ is trivial, since the edge of the sail is sunward and no thrust is produced. This case was numerically verified. For the non-trivial case we have the analytic equations:

$$\triangle a = -\frac{3}{4}a^{3/2}DT\sin(\phi-\gamma) \qquad (47)$$

$$\triangle e = 0 \qquad (48)$$

$$\triangle i = -\frac{a^{1/2}}{8}DT\sin(\phi-\gamma) \qquad (49)$$
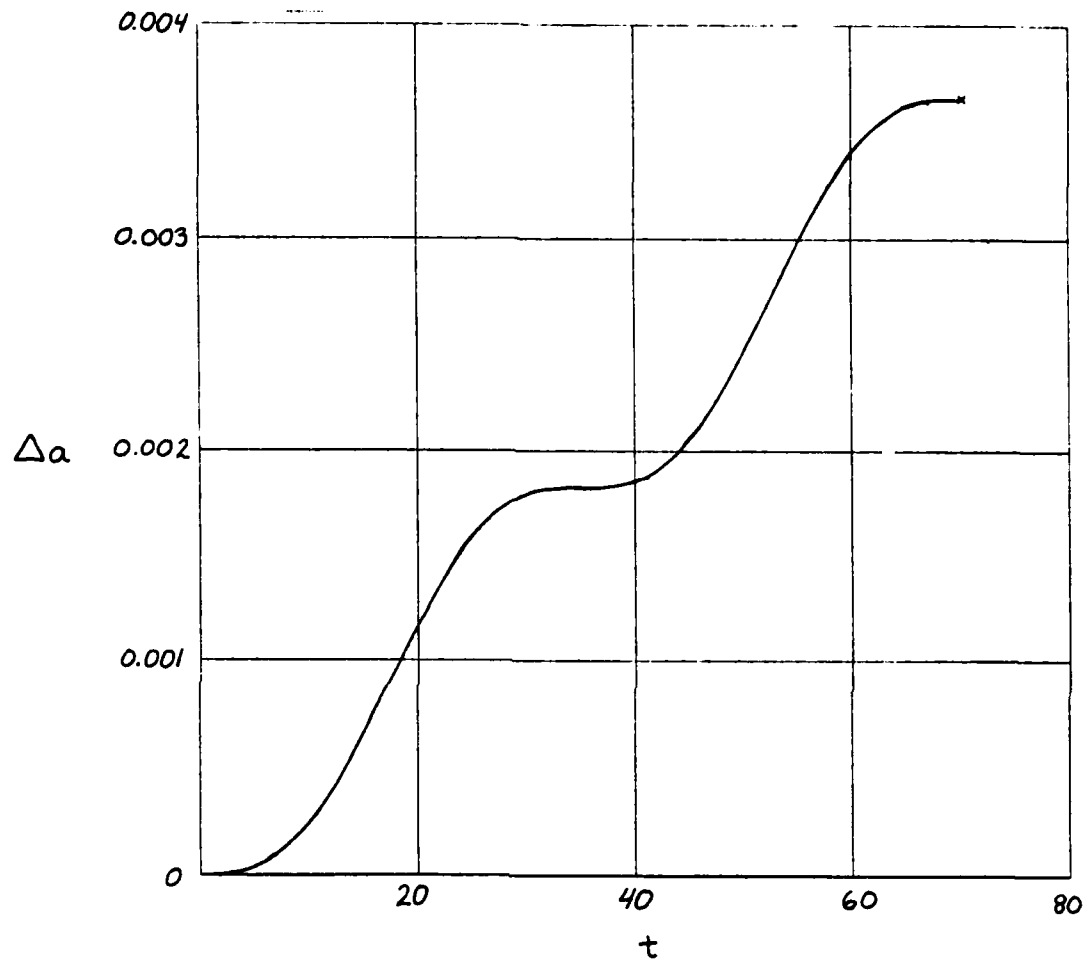
Fig 9. Δa vs t, Spinning Case

The interesting result is that both $\triangle a$ and $\triangle i$ vary with the sine of the phase angle difference. So for this case, changing $\triangle a$ implies changing $\triangle i$. This case was numerically verified and the results are shown in Figs 10 where the line is the variation over time and "x" marks the point predicted by Eqs 47-49.

Coning. The simple coning case has H directed at the sun and a nutation angle of one-fourth pi radians. The resulting analytical equations are:

$$\triangle a = \frac{\sqrt{2}}{4} a^{3/2} DT \cos(\phi - \gamma) \tag{50}$$

$$\triangle e = 0 \tag{51}$$

$$\triangle i = -\frac{\sqrt{2}}{4} a^{1/2} DT \sin(\phi - \gamma) \tag{52}$$

These equations indicate two important results. First, by selecting the phase angle difference to be in the fourth quadrant, both $\triangle a$ and $\triangle i$ can be positive. Second, and most important, by selection of the magnitude of the phase angle difference, it is possible to trade off $\triangle a$ for $\triangle i$ and vice versa. Any combination of $\triangle a$ and $\triangle i$ within the magnitudes given is possible. This includes, of course, selecting only $\triangle a$ or only $\triangle i$. Two cases were verified

- 37 -
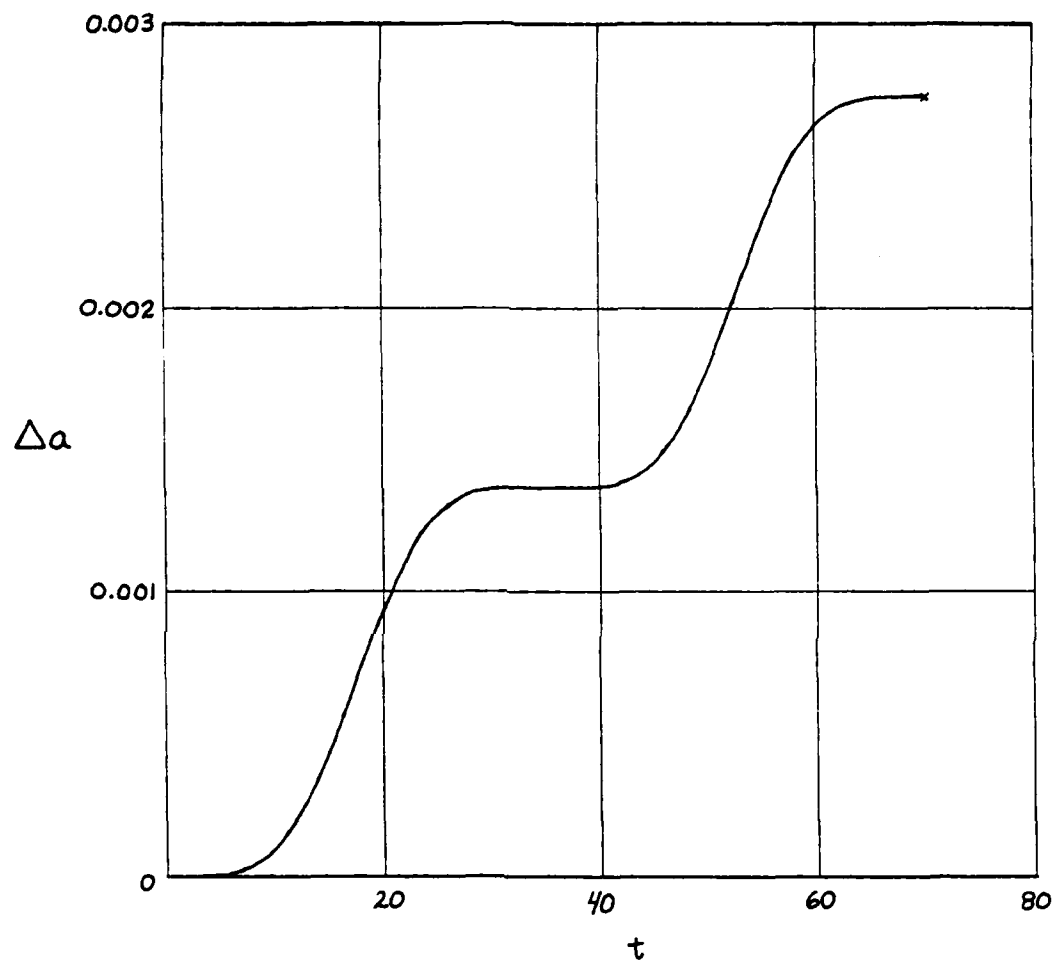
Fig 10a. Δa vs t, Tumbling Case
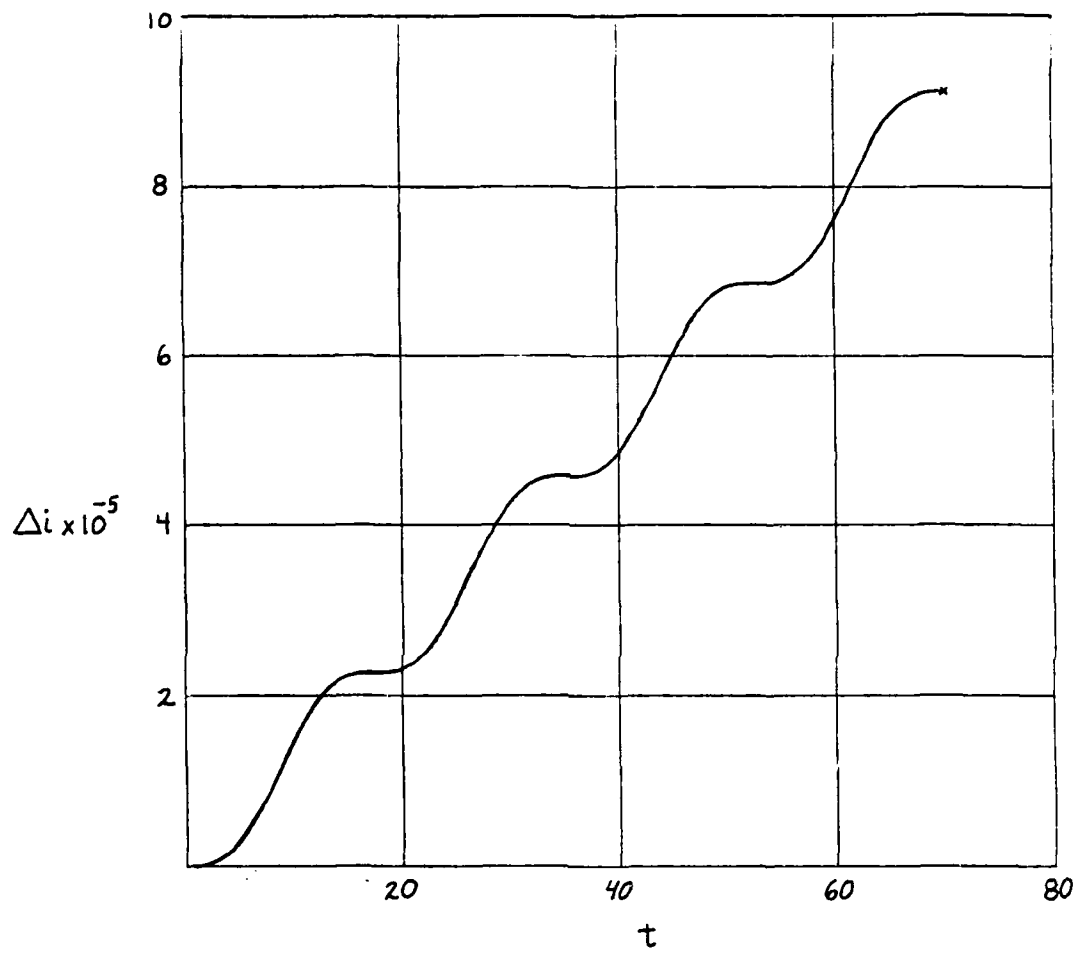
Fig 10b. $\triangle i$ vs t, Tumbling Case

numerically: the maximum $\triangle i$ case and the maximum $\triangle a$ case both showed excellent agreement between analytic and numeric solutions. The results are contained in Figs 11.

Motion in the Inclined Plane.

The next level of complexity is to consider cases in the inclined plane. This adds equations for the change in longitude of the ascending node. Initially, an inclination of thirty degrees was considered and the simple cases, with some variations, were considered.

Spinning. Two spinning cases were considered: case one with $\hat{H}$ parallel to $\hat{k}$ and case two with $\hat{H}$ perpendicular to $\hat{s}$ and $\hat{j}$. The analytical equations for case one are:

$$\triangle a = -\cos^2 i\, a^{3/2} D T \sin(\phi - \gamma) \qquad (53)$$

$$\triangle e = \triangle i = \triangle \Omega = 0 \qquad (54)$$

As expected, case one showed substantial change in $\triangle a$ (.274E-02 $DU_{\oplus}$) and no other changes. These are the analytical equations for case two:

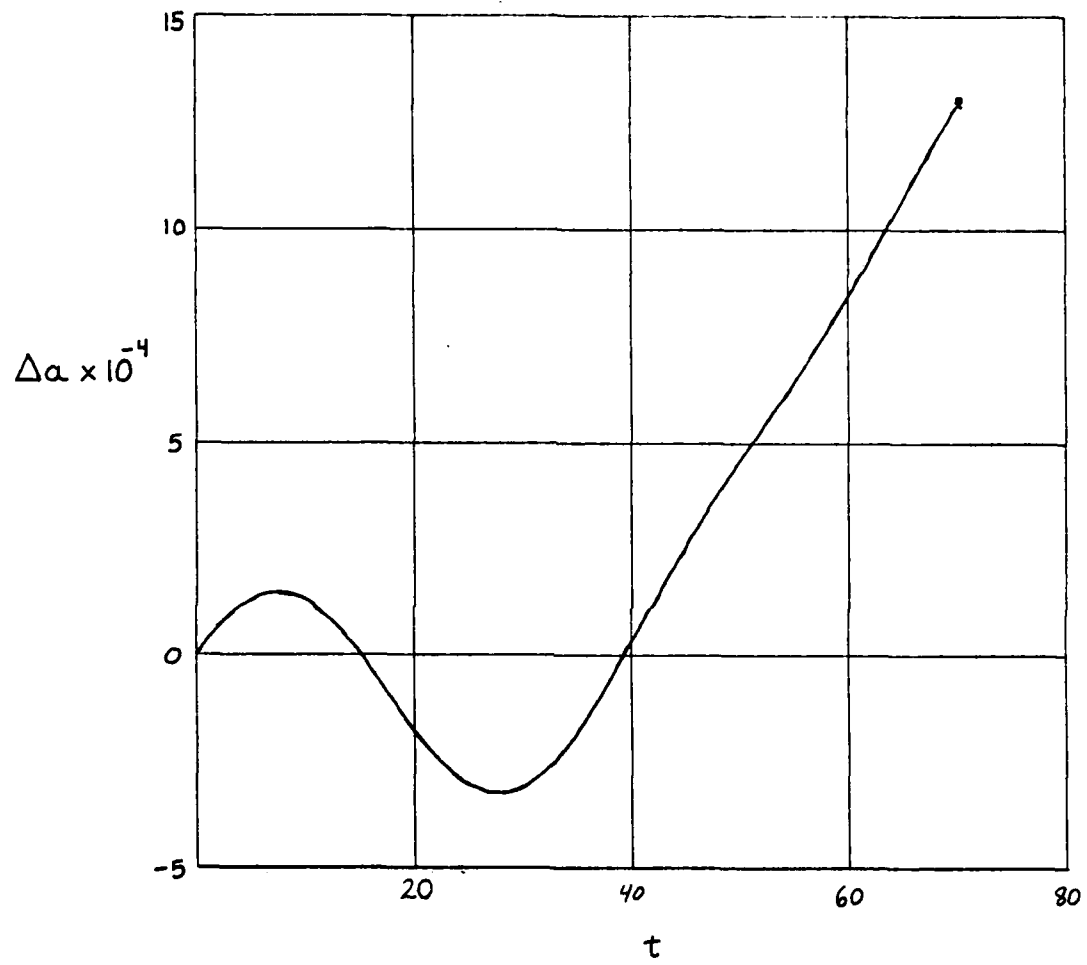$$\triangle a = \frac{(3\sqrt{3} + 2)}{8} a^{3/2} D T \cos(\phi - \gamma) \qquad (55)$$
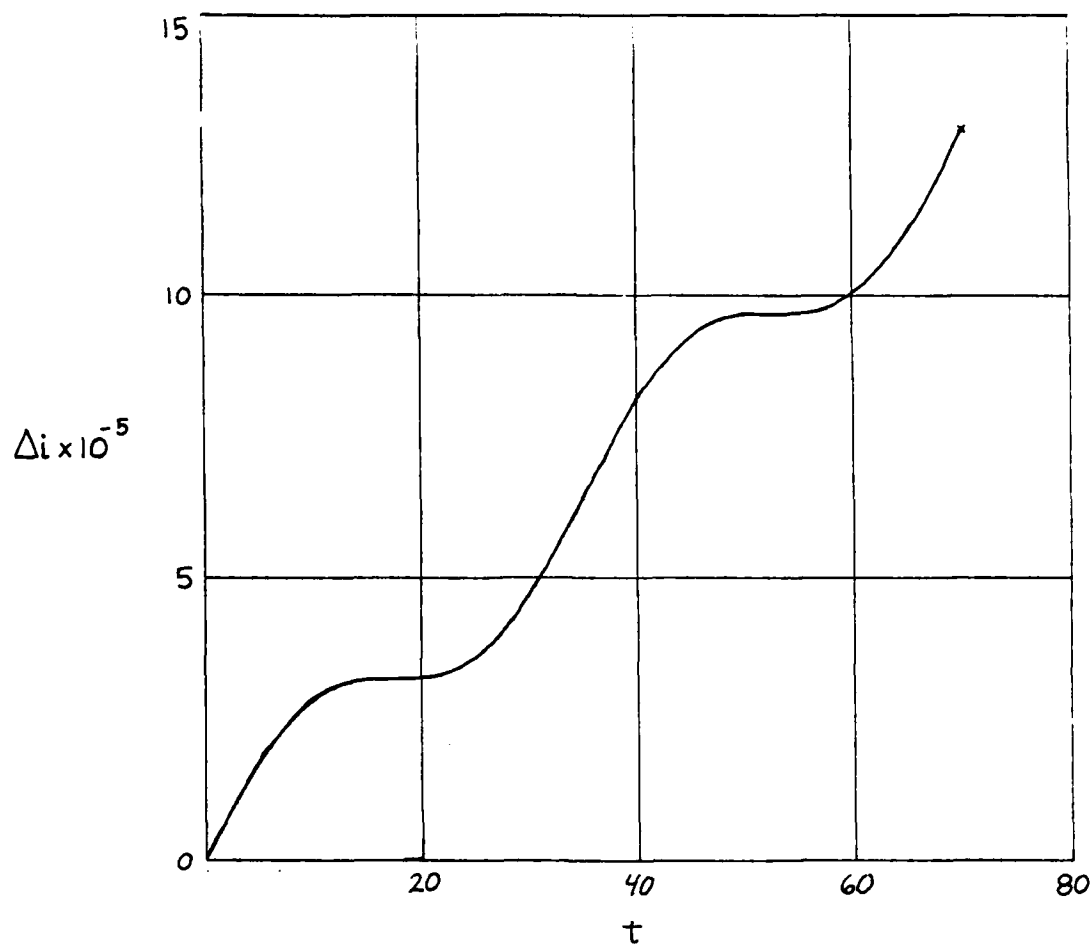
Fig 11a. Δa vs t, Coning Case

Fig 11b. Δi vs t, Tumbling Case

$$\triangle e = 0 \tag{56}$$

$$\triangle i = -\frac{3}{16} a^{\frac{1}{2}} DT \sin(\phi - \psi) \tag{57}$$

$$\triangle \Omega = \frac{3}{8} a^{\frac{1}{2}} DT \cos(\phi - \psi) \tag{58}$$

Case two featured a phase angle difference of negative one-half pi radians and so showed significant change in $\triangle i$ (.14E-03) and no other changes. This verifies the importance of the phase difference in determining the changes in the orbital parameters.

Tumbling. Two tumbling cases were considered: case one with $\hat{H}$ parallel to $\hat{j}$ and case two with $\hat{H}$ parallel to $\hat{i}$. The analytical equations for case one are:

$$\triangle a = \frac{a^{3/2}}{8} DT \left[\frac{3}{4} \cos(\phi - \psi) - 5 \sin(\phi - \psi) \right] \tag{59}$$

$$\triangle e = 0 \tag{60}$$

$$\triangle i = \frac{3}{16} a^{\frac{1}{2}} DT \sin(\phi - \psi) \tag{61}$$

$$\Delta \Omega = \frac{a^{1/2}}{8} DT \left[3\cos(\phi - \gamma) - \sqrt{3} \sin(\phi - \gamma) \right] \qquad (62)$$

Case one, with a phase angle difference of negative one-half pi radians, showed significant changes in Δa (.228E-2 $DU_\oplus$), Δi (.137E-3) and $\Delta \Omega$ (.158E-3). This indicates a possibility that similar cases could be used to provide a variety of changes in Δa, Δi and $\Delta \Omega$, depending on mission requirements. Case two analytical equations are:

$$\Delta a = \frac{a^{3/2}}{16} DT \cos(\phi - \gamma) \qquad (63)$$

$$\Delta e = 0 \qquad (64)$$

$$\Delta i = -\frac{3}{32} a^{1/2} DT \sin(\phi - \gamma) \qquad (65)$$

$$\Delta \Omega = \frac{3}{16} a^{1/2} DT \cos(\phi - \gamma) \qquad (66)$$

Case two was tested with the same phase angle difference as the previous cases, providing significant change in Δi (.685E-4) only. This strategy provides the option of changing i or a and Ω, or combinations of all

three.

Coning. Four cases of coning were considered: two each of case one ($\hat{H}$ parallel to $\hat{s}$) and two each of case two ($\hat{H}$ parallel to $\hat{i}$). In case one, phase angle differences were changed to test the case for maximizing Δa and Δi, and likewise for case two. The analytical equations for case one are:

$$\Delta a = \sqrt{2}\, a^{3/2} DT \cos(\phi - \gamma) \tag{67}$$

$$\Delta e = 0 \tag{68}$$

$$\Delta i = \sqrt{6}\, a^{1/2} DT \sin(\phi - \gamma) \tag{69}$$

$$\Delta \Omega = \frac{\sqrt{6}}{8}\, a^{1/2} DT \cos(\phi - \gamma) \tag{70}$$

The equations for case two are:

$$\Delta a = \left(\frac{8\sqrt{6} + 13\sqrt{2}}{64}\right) a^{3/2} DT \cos(\phi - \gamma) \tag{71}$$

- 45 -

$$\Delta e = \left(\frac{2 + \sqrt{6}}{128} \right) a^{\frac{1}{2}} DT \sin(2(\phi - \psi)) \qquad (72)$$

$$\Delta i = -\frac{15\sqrt{2}}{128} a^{\frac{1}{2}} DT \sin(\phi - \psi) \qquad (73)$$

$$\Delta \Omega = \frac{15\sqrt{2}}{64} a^{\frac{1}{2}} DT \cos(\phi - \psi) \qquad (74)$$

Case two proved slightly superior for changing Δi, (.121E-3 vs .112E-3) with no other orbital parameters changing. Case two also proved superior in the second phase angle difference case, giving superior performance in Δa (.217E-2 vs .646E-3 DU.), and $\Delta \Omega$ (.242E-3 vs .224E-3) with no other orbital parameters changing. Note that maximizing a involves maximizing Ω. Trade-offs can be made between Δa and Δi. Agreement between numeric and analytic results was excellent.

Arbitrary Cases. Three cases were tested in which phase, orientation, inclination and nutation angles were randomly determined. Agreement between numeric and analytic results was excellent. One such case is displayed in Figs 12.

Nutation Angle.

The search for the optimum nutation angle was accomplished on a case by case basis. The case of $\hat{H}$ pointing at the sun, inclination equals zero, yields an
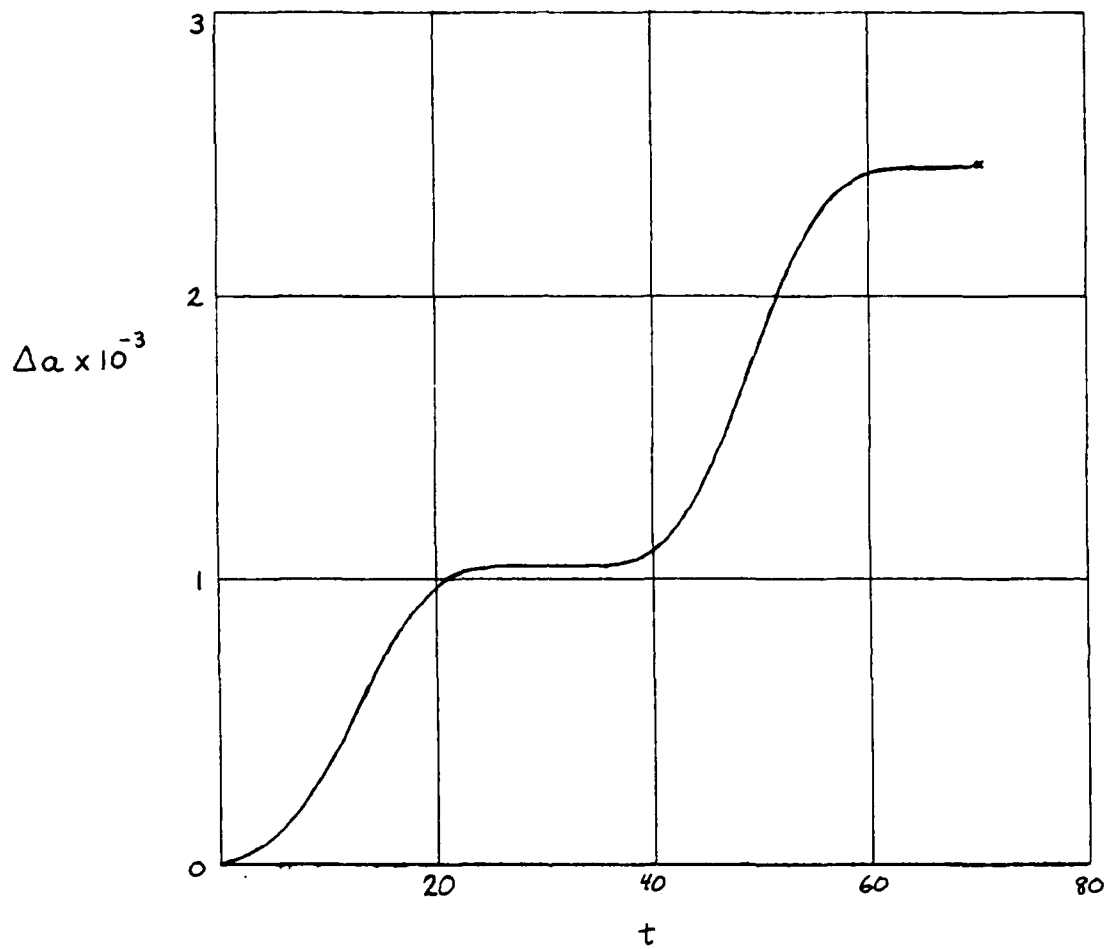
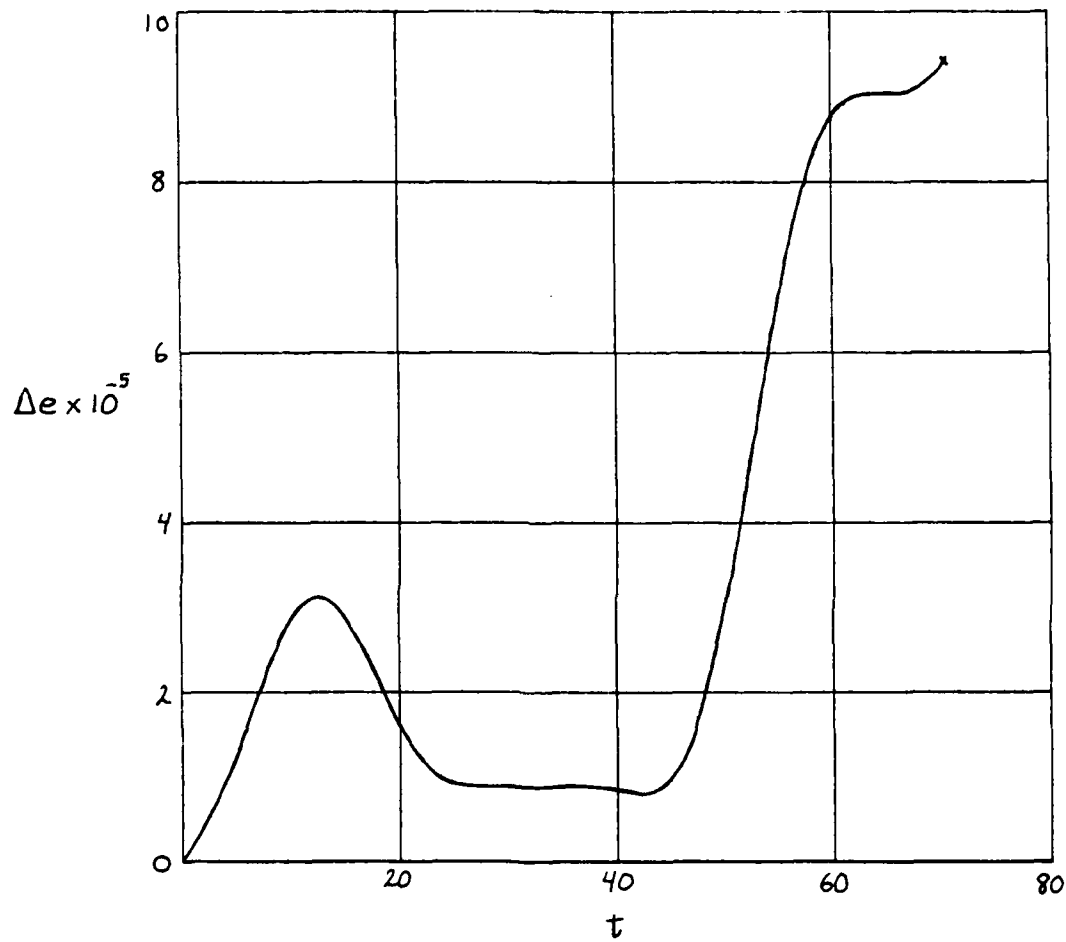Fig 12a. $\triangle$a vs t, Arbitrary Case

Fig 12b. Δe vs t, Arbitrary Case

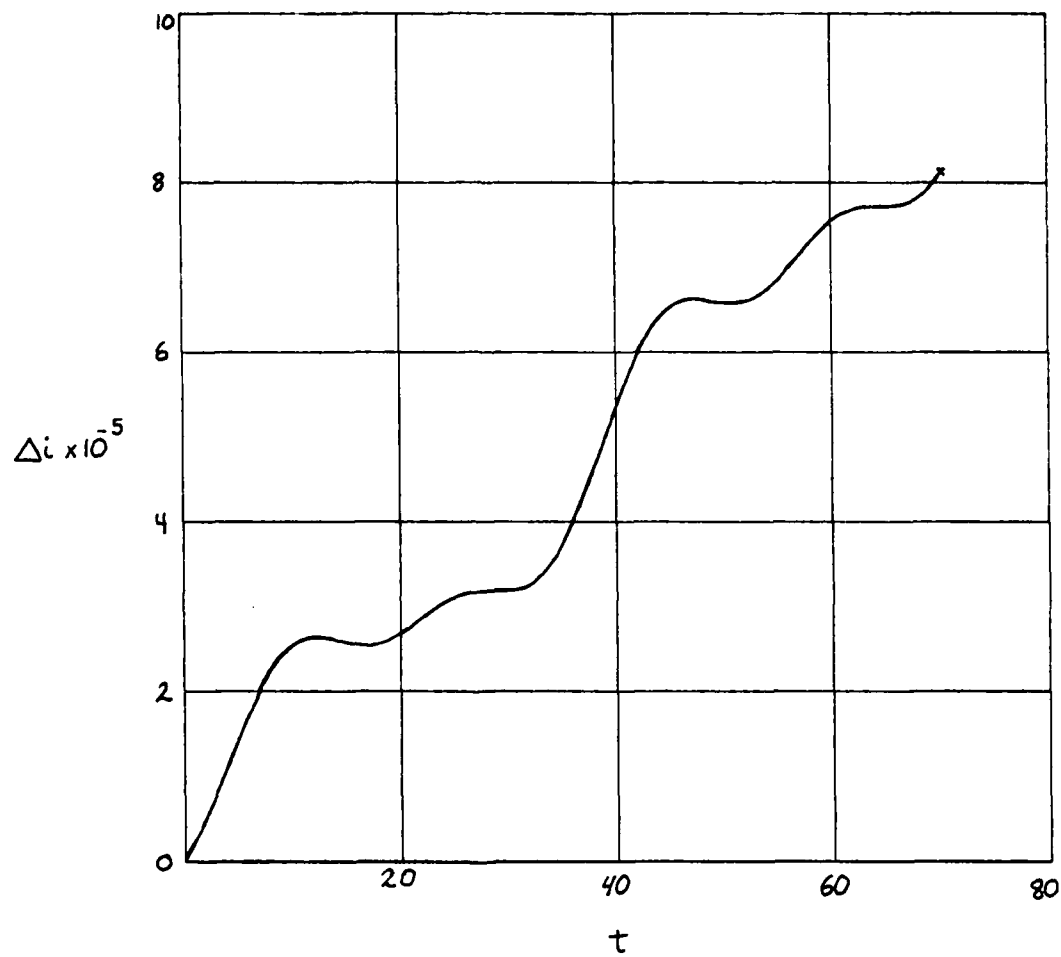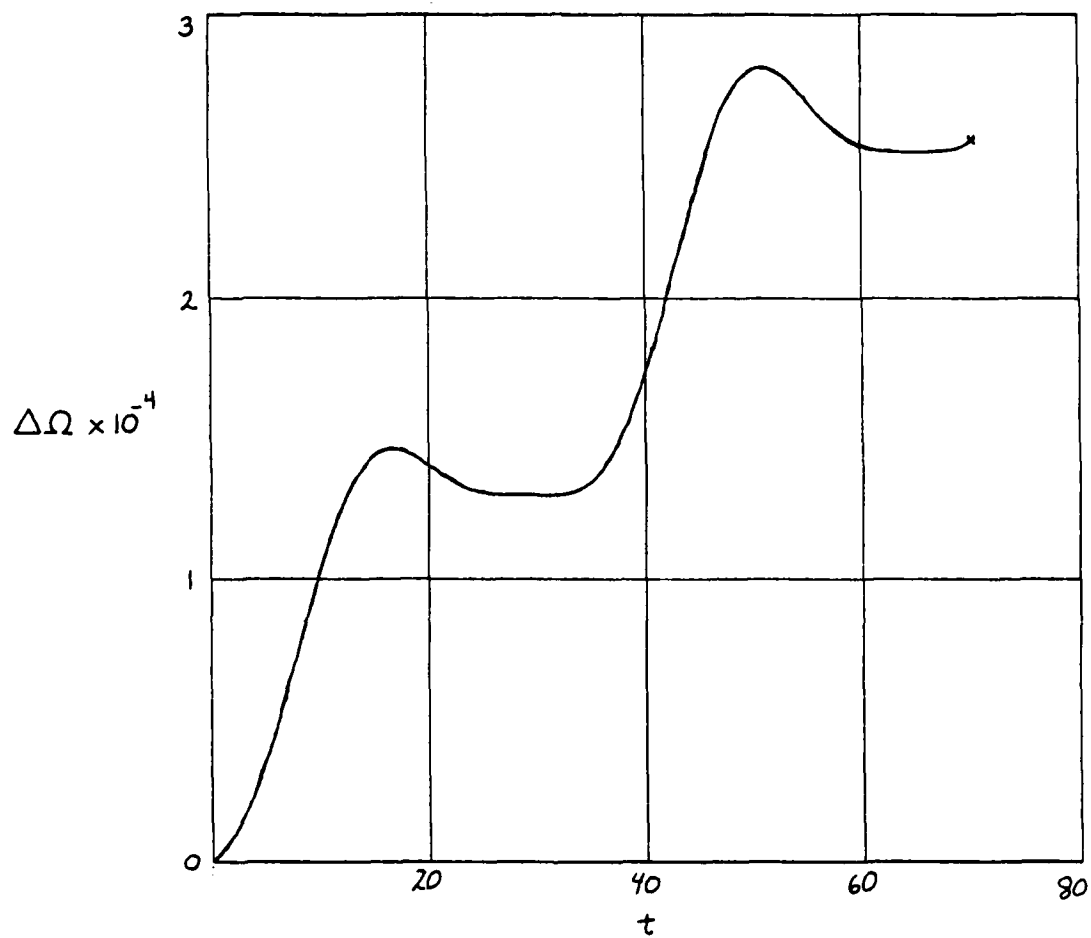Fig 12c. Δi vs t, Arbitrary Case

Fig 12d. $\Delta\Omega$ vs t, Arbitrary Case

optimum nutation angle of approximately 35.2 degrees. The

change in $\triangle$a as a function of θ for this case is shown in

Fig 13. For the 30 degree inclined case with $\hat{H}$ parallel to

$\hat{i}$, the optimum nutation angle is 35.2 degrees for increasing

$\triangle$a but is 40.2 degrees for maximizing $\triangle\Omega$. For the 30

degree inclined orbit with $\hat{H}$ parallel to $\hat{s}$, the optimum

nutation angle is again 35.2 degrees for changing $\triangle$a and

40.2 degrees for maximizing $\triangle$i. These are surprising

results, to say the least.

Limits of Validity.

A study of the variation of $\triangle$a with a was done to find

at what point the perturbation assumptions became invalid.

The study indicated a maximum change in $\triangle$a of 0.25 $DU_\oplus$ at

·10 $DU_\oplus$ for the spinning case. This will serve as an upper

bound on the usefulness of these equations.

Discussion.

Conclusions.

The spinning case is preferred for missions where

changing the semimajor axis is the only requirement. Few,

if any, such missions exist. This implies that correct

inclination was achieved at insertion into orbit, which

implies that impulsive power sources were used. The cost of

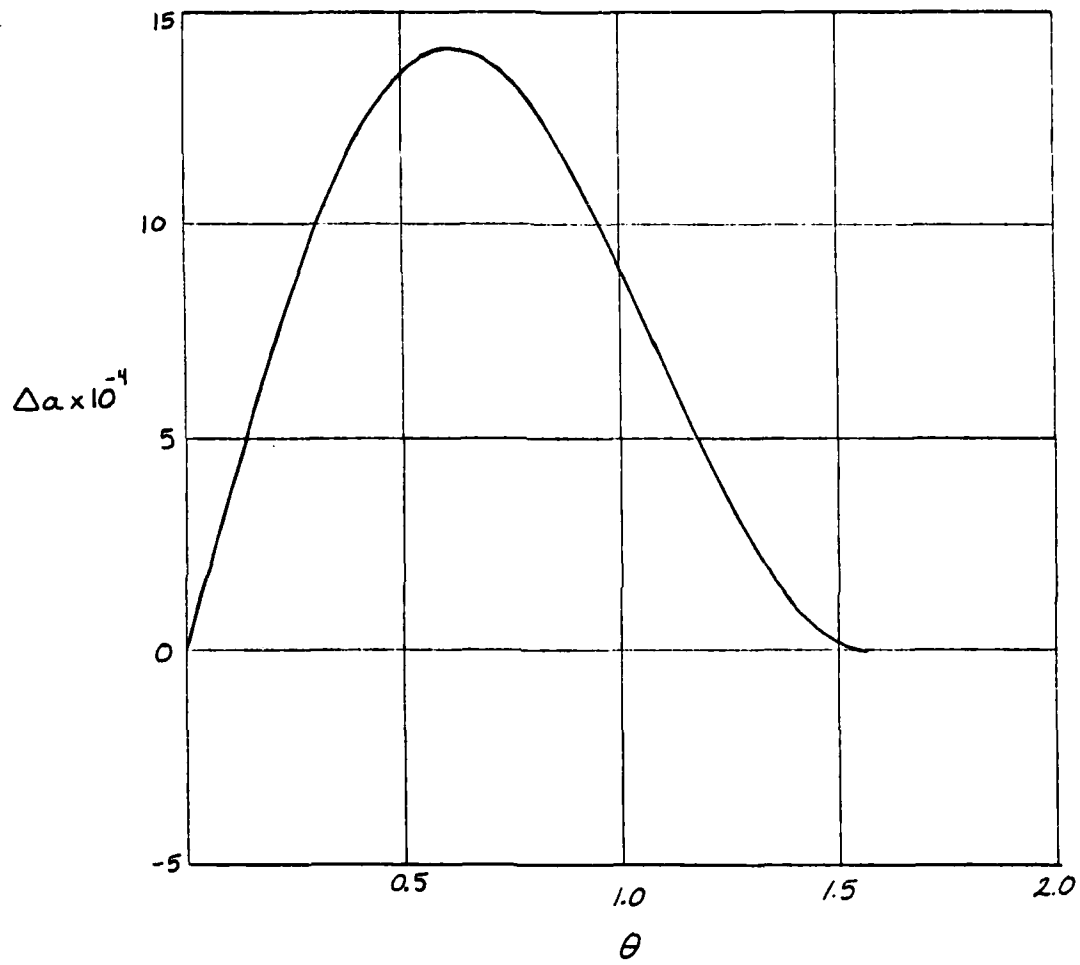such sources can be avoided by using the sails capability

Fig 13. $\triangle$a vs θ

for inclination changes.

The tumbling case is to be avoided unless mission requirements call for the ratio of $\triangle a/\triangle i$ inherent in such a strategy. This is unlikely.

The coning cases are the only ones which provide the opportunity to trade off $\triangle a$ for $\triangle i$. Any ratio of $\triangle a/\triangle i$ desired can be produced by adjusting the difference in the phase angles. Coning motion strategies thus compose a set of strategies of considerable practical interest.

The 35.2 degree nutation angle results are suspect until a more detailed study can be accomplished. It is possible that for the differences in the cases studied that the differences in the nutation angles were small enough to escape notice.

Directions for Further Study

More questions have been raised than have been answered. Besides the obvious point of investigating the optimum nutation angle in more detail, a host of other topics suggest themselves.

The many-orbit case needs investigation. This involves establishing an inertial reference frame in the plane of the ecliptic and updating many of the angles assumed constants in this study. Complex missions can thus be analyzed.

Including eccentricities not equal to zero will add much to the generality of the results, but the valiant soul who attempts this should be forwarned: the equations in $\triangle(e\sin\omega)$ and $\triangle(e\cos\omega)$ will be approximately forty hand-written pages each. This author made excursions in pursuit of this grail when the complexity of it was still cloaked in a sophomoric error. Note that this level of effort only gains enough terms to make consideration of eccentricities up to 0.01 possible. One might be well advised to find a dependable numerical method for such pursuits.

Other improvements would include adding the effects of eclipse to the study. This would consist of developing an algorithm which would give times of eclipse, integrating up to the boundary and then coasting through the eclipse. Another improvement would be considering sails which are less than perfectly specular.

Lastly, there are infinitely many cases to be investigated with the equations provided herein. Variation of the orbital parameters with i or with the resonance number would be a good jumping off spot for the curious. Can a function be found which gives the best angle between $\hat{H}$ and $\hat{s}$? The possibilities are endless.

Appendix A

General Perturbation Solutions

For simplicity of notation, the following two functions are defined:

$$C(a,b) = \frac{\cos((an+b\nu)T + a\phi + b\gamma) - \cos(a\phi - b\gamma)}{an + b\gamma} \tag{A1}$$

$$S(a,b) = \frac{\sin((an+b\nu)T + a\phi + b\gamma) - \sin(a\phi - b\gamma)}{an + b\gamma} \tag{A2}$$

where a and b are constants here.

Since these functions typically occur in pairs such as C(a,b), C(a,-b) it can easily be seen that the resonance condition is simply:

$$\nu = \frac{a}{b} n \tag{A3}$$

where a/b is the resonance number, designated "x" in the text.

The general perturbation solutions follow:

$$\Delta a = 2a^{3/2} D \Big[d_1^2 \Big(\tfrac{\beta_1}{8} \big[3C(1,1) + C(1,-1) + C(1,3) + C(1,-3) \big]$$

$$+ \tfrac{\beta_2}{8} \big[S(1,-3) - S(1,3) + S(1,-1) - S(1,1) \big] + \tfrac{\beta_3}{2} \big[C(1,0) + \tfrac{1}{2}(C(1,2) +$$

$$C(1,-2)) \big] + \tfrac{\beta_4}{8} \big[3S(1,-1) + S(1,1) + S(1,3) + S(1,-3) \big] + \tfrac{\beta_5}{8} \big[C(1,-1) -$$

$$C(1,1) + C(1,-3) - C(1,3) \big] + \tfrac{\beta_6}{2} \big[S(1,0) + \tfrac{1}{2}(S(1,-2) + S(1,2)) \big] \Big)$$

$$- 2d_1 d_2 \Big(-\tfrac{\beta_1}{8} \big[S(1,-3) - S(1,3) + S(1,-1) - S(1,1) \big] + \tfrac{\beta_2}{8} \big[-C(1,1) - C(1,-1)$$

$$+ C(1,3) + C(1,-3) \big] - \tfrac{\beta_3}{4} \big[S(1,-2) - S(1,2) \big] + \tfrac{\beta_4}{8} \big[C(1,-1) - C(1,1)$$

$$+ C(1,-3) - C(1,3) \big] + \tfrac{\beta_5}{8} \big[S(1,-1) + S(1,1) - S(1,-3) - S(1,3) \big] + \tfrac{\beta_6}{4}$$

$$\big[C(1,-2) - C(1,2) \big] \Big) + 2d_1 d_3 \Big(\tfrac{\beta_1}{2} \big[C(1,0) + \tfrac{1}{2}(C(1,2) + C(1,-2)) \big]$$

$$+ \tfrac{\beta_2}{4} \big[S(1,-2) - S(1,2) \big] + \tfrac{\beta_3}{2} \big[C(1,1) + C(1,-1) \big] + \tfrac{\beta_4}{2} \big[S(1,0) + \tfrac{1}{2}(S(1,-2)$$

$$+ S(1,2)) \big] + \tfrac{\beta_5}{4} \big[C(1,-2) - C(1,2) \big] + \tfrac{\beta_6}{2} \big[S(1,-1) + S(1,1) \big] \Big) - 2d_2 d_3$$

$$\Big(-\tfrac{\beta_1}{4} \big[S(1,-2) - S(1,2) \big] + \tfrac{\beta_2}{2} \big[-C(1,0) + \tfrac{1}{2}(C(1,2) + C(1,-2)) \big] -$$

$$\tfrac{\beta_3}{2} \big[S(1,-1) - S(1,1) \big] + \tfrac{\beta_4}{4} \big[C(1,-2) - C(1,2) \big] + \tfrac{\beta_5}{2} \big[S(1,0) - \tfrac{1}{2}($$

$$S(1,-2) + S(1,2)) \big] + \tfrac{\beta_6}{2} \big[C(1,-1) - C(1,1) \big] \Big) + d_2^2 \Big(-\tfrac{\beta_1}{8} \big[-C(1,1) - C(1,-1)$$

$$+ C(1,3) + C(1,-3) \big] + \tfrac{\beta_2}{8} \big[3(S(1,-1) - S(1,1)) - S(1,-3) + S(1,3) \big] -$$

$$\tfrac{\beta_3}{2} \big[-C(1,0) + \tfrac{1}{2}(C(1,2) + C(1,-2)) \big] + \tfrac{\beta_4}{8} \big[S(1,-1) + S(1,1) - S(1,-3)$$

$$- S(1,3) \big] + \tfrac{\beta_5}{8} \big[3(C(1,-1) - C(1,1)) + C(1,3) - C(1,-3) \big] + \tfrac{\beta_6}{2} \big[S(1,0) -$$

$$\tfrac{1}{2}(S(1,-2) + S(1,2)) \big] \Big) + d_3^2 \Big(\tfrac{\beta_1}{2} \big[C(1,1) + C(1,-1) \big] + \tfrac{\beta_2}{2} \big[S(1,-1) -$$

$$S(1,1)] + \beta_3 C(1,0) + \frac{\beta_4}{2}[S(1,-1)+S(1,1)] + \frac{\beta_5}{2}[C(1,-1)-C(1,1)]$$

$$+ \beta_6 S(1,0))] \tag{A4}$$

$$\Delta e = a^{1/2} D\Big[d_1^2 \Big(\frac{\beta_1}{16}[3(C(2,1)+C(2,-1))+C(2,3)+C(2,-3)]$$

$$+\frac{\beta_2}{16}[S(2,-3)-S(2,3)+S(2,-1)-S(2,1)] + \frac{\beta_3}{4}[C(2,0)+\tfrac12($$

$$C(2,2)+C(2,-2))]] + \frac{\beta_4}{8}[9S(0,1)+3S(0,3)+\tfrac12(3\{S(2,-1)+$$

$$S(2,1)\}+S(2,-3)+S(2,3))] + \frac{\beta_5}{8}[-3(C(0,3)+C(0,1))+\tfrac12($$

$$-C(2,3)+C(2,-3)-C(2,1)+C(2,-1))] + \frac{\beta_6}{4}[3(T+S(0,2))$$

$$+S(2,0)+\tfrac12(S(2,2)+S(2,2))]]\Big) -2d_1 d_2\Big(-\frac{\beta_1}{16}[S(2,-3)-S(2,3)$$

$$S(2,-1)-S(2,1)] + \frac{\beta_2}{16}[C(2,-3)+C(2,3)-C(2,1)-C(2,-1)]$$

$$-\frac{\beta_3}{8}[S(2,-2)-S(2,2)] + \frac{\beta_4}{8}[-3(C(0,3)+C(0,1))+\tfrac12(-C(2,3)+$$

$$C(2,-3)-C(2,1)+C(2,-1)] + \frac{\beta_5}{8}[3(S(0,1)-S(0,3))+\tfrac12(S(2,-1)$$

$$+S(2,1)-S(2,-3)-S(2,3)] + \frac{\beta_6}{4}[-3C(0,2)+\tfrac12(C(2,2)-C(2,2))]\Big)$$

$$+d_2^2\Big(-\frac{\beta_1}{16}[C(2,-3)+C(2,3)-C(2,1)-C(2,-1)] + \frac{\beta_2}{16}[3(S(2,-1)-$$

$$S(2,1))-S(2,-3)+S(2,3)] + \frac{\beta_3}{4}[-C(2,0)+\tfrac12(C(2,2)+C(2,-2))]$$

$$+\frac{\beta_4}{8}[3(S(0,1)-S(0,3))+\tfrac12(S(2,-1)+S(2,1)-S(2,-3)-S(2,3))]$$

$$+\frac{\beta_5}{8}[-9C(0,1)+3C(0,3)+\tfrac12(3\{-C(2,1)+C(2,-1)\}+C(2,3)-$$

$$C(2,-3))] + \frac{\beta_6}{4}[3(T - S(0,2)) + S(2,0) - \tfrac{1}{2}(S(2,-2) + S(2,2))]\Big)$$

$$+ 2d_1 d_3 \Big(\frac{\beta_1}{4}[C(2,0) + \tfrac{1}{2}(C(2,2) + C(2,-2))] + \frac{\beta_2}{8}[S(2,-2) - S(2,2)]$$

$$+ \frac{\beta_3}{4}[C(2,-1) + C(2,1)] + \frac{\beta_4}{4}[3(T + S(0,2)) + S(2,0) + \tfrac{1}{2}(S(2,-2)$$

$$+ S(2,2)] + \frac{\beta_5}{4}[-3C(0,2) + \tfrac{1}{2}(C(2,-2) - C(2,2))] + \frac{\beta_6}{2}[3S(0,1) +$$

$$\tfrac{1}{2}(S(2,-1) + S(2,1))]\Big) - 2d_2 d_3 \Big(-\frac{\beta_1}{8}[S(2,-2) - S(2,2)] + \frac{\beta_2}{4}[-C(2,0)$$

$$+ \tfrac{1}{2}(C(2,2) + C(2,-2))] - \frac{\beta_3}{4}[S(2,-1) - S(2,1)] + \frac{\beta_4}{4}[-3C(0,2) +$$

$$\tfrac{1}{2}(C(2,2) - C(2,2))] + \frac{\beta_5}{4}[3(T - S(0,2)) + S(2,0) - \tfrac{1}{2}(S(2,-2) +$$

$$S(2,2)] + \frac{\beta_6}{2}[-3C(0,1) + \tfrac{1}{2}(C(2,-1) - C(2,1))]\Big) + d_3^2 \Big(\frac{\beta_1}{4}[C(2,-1) +$$

$$C(2,1)] + \frac{\beta_2}{4}[S(2,-1) - S(2,1)] + \frac{\beta_3}{2}C(2,0) + \frac{\beta_4}{2}[3S(0,1) + \tfrac{1}{2}(S(2,-1)$$

$$+ S(2,1)] + \frac{\beta_5}{2}[-3C(0,1) + \tfrac{1}{2}(C(2,-1) - C(2,1))] + \frac{\beta_6}{2}[3T + S(2,0)]\Big)\Big]$$

$$\tag{A5}$$

$$\Delta i = a^{1/2} D\Big[d_1^2 \Big(\frac{\beta_7}{8}[-C(1,1) + C(1,-1) - C(1,3) + C(1,-3)] + \frac{\beta_8}{8}[$$

$$-C(1,1) - C(1,-1) + C(1,3) + C(1,-3)]\Big) - 2d_1 d_2 \Big(\frac{\beta_7}{8}[S(1,-1) + S(1,1) -$$

$$S(1,-3) - S(1,3)] + \frac{\beta_8}{4}[C(1,-2) - C(1,2)]\Big) + 2d_1 d_3 \Big(\frac{\beta_7}{4}[C(1,-2) - C(1,2)]$$

$$+ \frac{\beta_8}{2}[S(1,-1) + S(1,1)]\Big) - 2d_2 d_3 \Big(\frac{\beta_7}{2}[S(1,0) - \tfrac{1}{2}(S(1,-2) + S(1,2))]$$

$$+ \frac{\beta_8}{2}[C(1,-1) - C(1,1)]\Big) + d_2^2 \Big(\frac{\beta_7}{8}[3(C(1,-1) - C(1,1)) + C(1,3) -$$

$$C(1,-3)] + \frac{\beta_8}{2}[S(1,0) - \tfrac{1}{2}(S(1,-2) + S(1,2))]\Big) + d_3^2 \Big(\frac{\beta_7}{2}[C(1,-1) -$$

$$C(1,1)] + \beta_8\, S(1,0)\Big) \tag{A6}$$

$$
\begin{aligned}
\Delta\Omega = a^{1/2}\,D\,\mathrm{csci}\Big[\, & d_1^2\Big(\tfrac{\beta_7}{8}\big[\,S(1,-3)-S(1,3)+S(1,-1)-S(1,1)\big] - \\
& \tfrac{\beta_8}{2}\big[C(1,0)+\tfrac{1}{2}\big(C(1,2)+C(1,-2)\big)\big]\Big) - 2d_1 d_2\Big(\tfrac{\beta_7}{8}\big[-C(1,1)- \\
& C(1,-1)+C(1,3)+C(1,-3)\big] + \tfrac{\beta_8}{2}\big[-C(1,0)+\tfrac{1}{2}\big(C(1,2)-C(1,-2)\big)\big]\Big) \\
& + d_2^2\Big(\tfrac{\beta_7}{8}\big[3\big(S(1,-1)-S(1,1)\big)-S(1,-3)+S(1,3)\big]+\tfrac{\beta_8}{2}\big[-C(1,0) \\
& +\tfrac{1}{2}\big(C(1,2)+C(1,-2)\big)\big]\Big) + 2d_1 d_3\Big(\tfrac{\beta_7}{4}\big[S(1,-2)-S(1,2)\big]-\tfrac{\beta_8}{2}\big[\\
& C(1,1)+C(1,-1)\big]\Big) - 2d_2 d_3\Big(\tfrac{\beta_7}{2}\big[C(1,0)+\tfrac{1}{2}\big(C(1,2)+C(1,-2)\big)\big] \\
& +\tfrac{\beta_8}{2}\big[S(1,-1)-S(1,1)\big]\Big) + d_3^2\Big(\tfrac{\beta_7}{2}\big[S(1,-1)-S(1,1)\big]-\beta_8\,C(1,0)\big)\Big]
\end{aligned}
\tag{A7}
$$

Appendix B

Haming

```
      subroutine haming(nxt)
c     Haming is an ordinary diferential equation integrator.
c     x is the independent variable, in our case: time.
c     y is the state vector.
c     f is the right hand sides of the differential equations
c       to be integrated. f is explicity defined in a user-written
c       subroutine called rhs.
c     errest is an error estimate.
c     n is the number of ordinary differential equations.
c     h is the step size.
c
c
c
c     ham must be in the calling program and in rhs.
c     The first array parameter of y and f in ham is the
c     number of ODEs.
c     The first call on Haming is with n=0,nxt=1,y at initial
c     values,n=#of ODEs. h is one ith of a period and h is only
c     called 101 times. to complete one period
c     (Ref 10)
c
      common /ham/ x,y(3,4),f(3,4),errest(3),n,h
      tol = 0.000001
      if(nxt) 100,10,200
  10  xo = x
      hh = h/2.0
      call rhs(1)
      do 40 l = 2,4
      x = x + hh
      do 20 i = 1,n
  20  y(i,l) = y(i,l-1) + hh*f(i,l-1)
      call rhs(l)
      x = x + hh
      do 30 i = 1,n
  30  y(i,l) = y(i,l-1) + h*f(i,l)
  40  call rhs(l)
      jsw = -10
  50  isw = 1
      do 120 i = 1,n
      hh = y(i,1) + h*( 9.0*f(i,1) + 19.0*f(i,2) - 5.0*f(i,3)
     1      + f(i,4) ) / 24.0
      if( abs(( hh - y(i,2))/(f(i,2)*h)).lt. tol ) go to 70
      isw = 0
  70  y(i,2) = hh
      hh = y(i,1) + h*( f(i,1) + 4.0*f(i,2) + f(i,3))/6.0
      if( abs(( hh-y(i,3))/(f(i,3)*h)).lt. tol ) go to 90
      isw = 0
  90  y(i,3) = hh
      hh = y(i,1) + h*( 3.0*f(i,1) + 9.0*f(i,2) + 9.0*f(i,3)
     1      + 3.0*f(i,4) ) / 8.0
      if( abs((hh-y(i,4))/(f(i,4)*h)).lt. tol ) go to 110
      isw = 0
 110  y(i,4) = hh
 120  continue
      x = xo
      do 130 l = 2,4
      x = x + h
 130  call rhs(l)
      if(isw) 140,140,150
 140  jsw = jsw + 1
      if(jsw) 50,280,230
 150  x = xo
      isw = 1
      jsw = 1
```

```fortran
      do 160 i = 1,n
160   errest(i) = 0.0
      nxt = 1
      go to 200
190   jsw = 2
      nxt = iabs(nxt)
200   x = x + h
      np1 = mod(nxt,4) + 1
      go to (210,230),isw
210   go to (270,270,270,220),nxt
220   isw = 2
230   nm2 = mod(np1,4) + 1
      nm1 = mod(nm2,4) + 1
      npo = mod(nm1,4) + 1
      do 240 i = 1,n
      f(i,nm2) = y(i,np1) + 4.0*h*( 2.0*f(i,npo) - f(i,nm1)
     1         + 2.0*f(i,nm2) ) / 3.0
240   y(i,np1) = f(i,nm2) - 0.925619835*errest(i)
      call rhs(np1)
      do 250 i = 1,n
      y(i,np1) = ( 9.0*y(i,npo) - y(i,nm2) + 3.0*h*( f(i,np1)
     1         + 2.0*f(i,npo) - f(i,nm1) ) ) / 8.0
      errest(i) = f(i,nm2) - y(i,np1)
250   y(i,np1) = y(i,np1) - 0.0743801653 * errest(i)
      go to (260,270),jsw
260   call rhs(np1)
270   nxt = np1
280   return
      end
```

Bibliography

1. Alfano, S. "Low Thrust Orbit Transfer," AFIT Thesis AFIT/GA/AA/82D-2, WPAFB, Ohio, 1982

2. Danby, J.M.A. _Fundamentals of Celestial Mechanics_. New York: MacMillan Publishing Co., Inc., 1962

3. Fimple, W.R., "Generalized Three-Dimensional Trajectory Analysis of Planetary Escape by Solar Sail," _Journal of the American Rocket Society_, Vol. 32, No. 6, 1962, pp. 883-887.

4. Garwin, R.L., "Solar Sailing - A Practical Method of Propulsion Within the Solar System," _Jet Propulsion_, Vol. 28, No. 3, March 1958, pp. 188-190.

5. Kaplan, M.H. _Modern Spacecraft Dynamics and Control_. New York: John Wiley & Sons, 1976

6. London, H.S., "Some Exact Solutions of the Equations of Motion of a Solar Sail with Constant Sail Setting," _Journal of the American Rocket Society_, Vol. 30, No. 2, 1960, pp.198-200.

7. Sands, N., "Escape from Planetary Gravitational Fields by Use of Solar Sails," _Journal of the American Rocket Society_, Vol. 31, No. 4, 1961, pp. 527-531.

8. Tsu, T.C., "Interplanetary Travel by Solar Sail," _Journal of the American Rocket Society_, Vol. 29, No. 6,

1959, pp. 422-427.

9. Van der Ha, J.C. and Modi, V.J. "Solar Pressure Induced Orbital Perturbations and Control of a Satellite in an Arbitrary Geocentric Trajectory," AIAA Aerospace Sciences Meeting, 15th, Los Angeles, CA, 24-26 Jan 1977, AIAA Paper No. 77-32.

10. Wiesel, W. unpublished notes, 1983

VITA

Keith L. Jenkins was born on 12 March 1951 in Keene, New Hampshire. He graduated from high school in Boiceville, New York in 1969 and attended Duke University from which he received the degree of Bachelor of Arts in Political Science and Religion in May 1973. He enlisted in the Air Force in February 1975 and received from the Community College of the Air Force an Associate in Applied Sciences degree in Radar Avionics Technology in April 1977. In June 1977 he entered the University of Colorado School of Engineering under the auspices of the Airman Education and Commissioning Program. He received a Bachelor in Engineering Sciences in Aerospace Engineering in December 1979, graduating as a member of Tau Beta Pi and Sigma Gamma Tau. After graduating with distinction from OTS, 2Lt. Jenkins served as a Satellite Test Engineer and Field Program Manager with the 6595th Aerospace Test Group, Vandenberg AFB, CA., until entering the School of Engineering, Air Force Institute of Technology in June 1982.

> Permanent address: 809 Picket Place
>
> Dayton, Ohio 45433

REPORT DOCUMENTATION PAGE

1a. REPORT SECURITY CLASSIFICATION Unclassified	1b. RESTRICTIVE MARKINGS
2a. SECURITY CLASSIFICATION AUTHORITY	3. DISTRIBUTION/AVAILABILITY OF REPORT Approved for public Release, Unlimited didtribution
2b. DECLASSIFICATION/DOWNGRADING SCHEDULE	

4. PERFORMING ORGANIZATION REPORT NUMBER(S) AFIT/GA/AA/83D-3	5. MONITORING ORGANIZATION REPORT NUMBER(S)

6a. NAME OF PERFORMING ORGANIZATION School of Engineering Air Force Institute of Technology	6b. OFFICE SYMBOL (If applicable)	7a. NAME OF MONITORING ORGANIZATION

6c. ADDRESS (City, State and ZIP Code) Air Force Institute of Technology Wright-Patterson AFB, OH 45433	7b. ADDRESS (City, State and ZIP Code)

8a. NAME OF FUNDING/SPONSORING ORGANIZATION	8b. OFFICE SYMBOL (If applicable)	9. PROCUREMENT INSTRUMENT IDENTIFICATION NUMBER

8c. ADDRESS (City, State and ZIP Code)	10. SOURCE OF FUNDING NOS.			
	PROGRAM ELEMENT NO.	PROJECT NO.	TASK NO.	WORK UNIT NO.

11. TITLE (Include Security Classification) See Box 19

12. PERSONAL AUTHOR(S) Keith L. Jenkins, First Lieutenant, USAF

13a. TYPE OF REPORT MS Thesis	13b. TIME COVERED FROM _____ TO _____	14. DATE OF REPORT (Yr., Mo., Day) 83 DEC	15. PAGE COUNT 73

16. SUPPLEMENTARY NOTATION

Approved for public release: IAW AFR 190-17.

13 JAN 1984

Lynn Walawn
LYNN E. WOLAVER
Dean for Research and Professional Development
Air Force Institute of Technology (ATC)

17. COSATI CODES			18. SUBJECT TERMS (Continue on reverse if necessary and identify by block number)
FIELD	GROUP	SUB. GR.	Solar Sailing, Low-Thrust Propulsion, Orbit Transfer,
3	3		Coning Motion, Orbital Perturbations
22	3		

19. ABSTRACT (Continue on reverse if necessary and identify by block number)

Title: The Orbital Motion of a Freely Coning Solar Sail

Thesis Chairman: Dr. William Wiesel

20. DISTRIBUTION/AVAILABILITY OF ABSTRACT UNCLASSIFIED/UNLIMITED ☒ SAME AS RPT. ☐ DTIC USERS ☐	21. ABSTRACT SECURITY CLASSIFICATION Unclassified

22a. NAME OF RESPONSIBLE INDIVIDUAL Dr. William Wiesel	22b. TELEPHONE NUMBER (Include Area Code) 513 255 2104	22c. OFFICE SYMBOL AFIT/ENY

DD FORM 1473, 83 APR EDITION OF 1 JAN 73 IS OBSOLETE.

This paper adresses orbital perturbations in the two-body problem of an Earth-orbiting solar sail undergoing free coning motion in a circular orbit. The coning motion controls both the magnitude and direction of the solar radiation pressure force. The equations of motion are expanded from the Lagrange planetary equations in their acceleration form and are solved assuming small changes in the orbital elements over the period of one orbit.

Resonances are observed between the mean motion of the sail and its precession rate. The one-to-one resonance case is examined and numerical methods are employed to verify the analytic results for the circular orbit case.

END

FILMED

2-84

DTIC